Abdullah, Zuraidah and Bayraktutan, Ulvi (2014) NADPH oxidase mediates TNF-α-evoked in vitro brain barrier dysfunction: roles of apoptosis and time. Molecular and Cellular Neuroscience, 61 . pp. 72-84. ISSN 1044-7431

Inhibition of TNF-α protects *in vitro* brain barrier from ischaemic damage

Cover title: Inhibition of TNF-α protects brain barrier

Zuraidah Abdullah, PhD; Kamini Rakkar, MSc; Philip MW Bath, MD; Ulvi Bayraktutan, PhD

Stroke, Division of Clinical Neuroscience, University of Nottingham, UK

Address for correspondence

Dr Ulvi Bayraktutan

Stroke, Division of Clinical Neuroscience,

School of Medicine,

Hucknall Road,

Nottingham NG5 1PB

UK

Tel: +44-(115)8231764

Fax: +44-(115)8231767

E-mail: ulvi.bayraktutan@nottingham.ac.uk

Word count: 7901

Abstract

Cerebral ischaemia, associated with neuroinflammation and oxidative stress, is known to perturb blood-brain barrier (BBB) integrity and promote brain oedema formation. Using an *in vitro* model of human BBB composed of brain microvascular endothelial cells and astrocytes, this study examined whether suppression of TNF-α, a potent pro-inflammatory cytokine, might attenuate ischaemia-mediated cerebral barrier damage. Radical decreases in transendothelial electrical resistance and concomitant increases in paracellular flux across co-cultures exposed to increasing periods of oxygen-glucose deprivation alone (0.5-20 h) or followed by 20 h of reperfusion (OGD±R) confirmed the deleterious effects of ischaemic injury on cerebral barrier integrity and function which concurred with reductions in tight junction protein (claudin-5 and occludin) expressions. OGD±R elevated TNF-α secretion, NADPH oxidase activity, $O_2^{\cdot-}$ production, actin stress fibre formation, MMP-2/9 activities and apoptosis in both endothelial cells and astrocytes. Increases in MMP-2 activity were confined to its extracellular isoform and treatments with OGD+R in astrocytes where MMP-9 could not be detected at all. Co-exposure of individual cell lines or co-cultures to an anti-TNF-α antibody dramatically diminished the extent of OGD±R-evoked oxidative stress, morphological changes, apoptosis, MMP-2/9 activities while improving the barrier function through upregulation of tight junction protein expressions. In conclusion, vitiation of the exaggerated release of TNF-α may be an important therapeutic strategy in preserving cerebral integrity and function during and following a cerebral ischaemic attack.

Keywords: TNF-α, ischaemic injury, cerebral barrier, *in vitro* model of BBB, NADPH oxidase, MMP.

Introduction

Ischaemic strokes emerging from an interference with blood supply to the central nervous system are characterised by disruption of the blood-brain barrier (BBB) and ensuing formation of brain oedema which constitute the leading cause of death within the first week after a stroke. The BBB consists of brain microvascular endothelial cells (BMEC), capillary basement membrane and astrocyte end-feet that control the exchange of molecules between the systemic circulation and the brain (Ballabh et al., 2004; Hayashi et al., 2004). As the presence of tight junctions (TJ), formed between adjacent endothelial cells via a series of intricate interactions between actin cytoskeleton and the major transmembrane and associated cytoplasmic proteins like claudin-5, occludin and zonula occludens-1, determines the overall BBB integrity and function, all intrinsic, extrinsic or humoral pathologies capable of affecting the appropriate construction of these junctional complexes will unavoidably affect the permeability of BBB (Dejana, 2004; Farrall and Wardlaw, 2009; Sandoval and Witt, 2008). Post-ischaemic neuroinflammation accompanied by exaggerated synthesis of pro-inflammatory cytokines has long been considered a central feature in cerebral barrier dysfunction. Indeed, excessive release of several cytokines, notably TNF-α, by infiltrated leukocytes and resident microglia during and/or after a cerebral attack is closely implicated in BBB breakdown through successive inductions of the most potent pro-oxidant and basement membrane-degrading enzymes, namely NADPH oxidase and matrix metalloproteinases (MMPs), respectively (Candelario-Jalil et al., 2009; Gao et al., 2008; Yang et al., 1999).

Immediately after focal ischaemia, a series of events including oxidative stress characterised by excessive availability of superoxide anion ($O_2^{\cdot -}$) occur. Once generated, $O_2^{\cdot -}$ evokes endothelial barrier failure in a direct fashion and through induction of BBB-related cell apoptosis (Basuroy et al., 2006). Other than reoxygenation of ischaemic tissue during reperfusion, activation of NADPH oxidase also significantly contributes to TNF-α-mediated overproduction of $O_2^{\cdot -}$ in vasculature (Chen et al., 2011; Gao et al., 2008; Zhang et al., 2006).

NADPH oxidase is composed of several cytosolic subunits and two membrane-bound components i.e. gp91-phox and p22-phox that are required for enzymatic activity and stability as a whole. Recent evidence have shown that both endothelial cells and astrocytes express all these subunits where efficacious suppression of oxidase activity via various structurally-distinct inhibitors like apocynin or minocycline improves cerebrovascular integrity after transient occlusion of middle cerebral artery by attenuating $O_2^{\cdot -}$ generation, endothelial dysfunction, BBB breakdown and the volume of brain oedema (Abdullah and Bayraktutan, 2014; Chen et al., 2009; Kahles et al., 2007; Williams et al., 2010).

Ischaemia-evoked induction of MMPs which lead to dissolution of extracellular matrix and basement membrane may also contribute to TNF-α-evoked BBB damage (Muhs et al., 2003; Parks et al., 2004). Aberrant endothelial cell anchoring and impaired matrix-endothelial cell signal transduction stemming from digestion of the structural support is likely to exacerbate the barrier damage. Indeed, a close correlation between TNF-α-evoked overexpression of MMP-2/9 and the extent of BBB openings has recently been shown in an experimental setting of focal cerebral ischaemia (Gasche et al., 1999; Rosenberg et al., 1998).

In light of the above, this study investigated the specific role of TNF-α in OGD±R-evoked BBB dysfunction with particular regards to modulations of NADPH oxidase, TJ protein expressions, MMP activity, cytoskeletal reorganisation and apoptosis using BMEC and astrocytes simultaneously.

Materials and Methods

All chemicals used during this study were from Sigma (Dorset, UK) unless otherwise stated.

Cell culture

Human BMEC (HBMEC) and astrocytes (HA) were purchased from TCS CellWorks Ltd (Buckingham, UK) and cultured in their respective specialised media (Sciencell Research Laboratories, San Diego, USA) in a humidified atmosphere (75% N_2, 20% O_2, 5% CO_2) at

37ºC. The EC media were supplemented with 5% foetal bovine serum, 1% penicillin/streptomycin mix and 1% endothelial growth supplement while the astrocyte media were supplemented with 2% foetal bovine serum, 1% penicillin/streptomycin mix and 1% astrocyte growth supplement. In some experiments, cells cultured to ~90% confluence and exposed to 4 h of OGD alone (94.95% N_2, 0.05% O_2, 5% CO_2) or followed by 20 h of reperfusion (OGD±R). All OGD experiments were performed using the D-glucose free medium (RPMI 1640, Invitrogen) and an MCO-18M multi-gas incubator (Sanyo, UK) flushed with N_2. O_2 levels were checked using an oxygen fyrite test kit (LEEC, UK) before use. Reperfusion was initiated by returning cells to normoxic conditions after changing the OGD media with the respective specialised media. In other experiments, the cells, in addition to OGD±R, were also exposed to an anti-TNF-α antibody (R&D Systems, Abingdon, UK). The antibody was added to the cells at the beginning of OGD and reperfusion for OGD alone and OG+R experiments, respectively.

Since both HBMEC and HA retain their BBB-specific properties at earlier passages, all the outlined experiments were performed using cells cultured up to and including passage 6 (Gu et al., 2003; Hurwitz et al., 1993; Kim et al., 2003).

***In vitro* model of human BBB**

Given that the contact HBMEC and HA co-culture model represents one of the better *in vitro* models of human BBB, this particular model was used during this study (Allen et al., 2010; Allen and Bayraktutan, 2009; Shao and Bayraktutan, 2013; Srivastava et al., 2013). In brief, approximately $75x10^3$ HA were seeded onto the outer surface of Transwell inserts (polyester membrane, 12 mm diameter, 0.4 µm pore size, Corning Costar, High Wycombe, UK) directed upside down in a 6-well tissue culture plate and allowed to adhere to the membrane overnight. The inserts were then inverted the correct way and placed in a sterile 12-well tissue culture plate containing fresh medium to grow to ~80% confluence. HBMEC (~$5x10^4$ cells) were then

added to the inner part of the membrane and both cell layers were grown to full confluence and maintained thereafter in their respective specialised media.

BBB experiments

The integrity and function of the BBB were studied by assessments of transendothelial electrical resistance (TEER) and paracellular flux of low (sodium fluorescein (NaF), Mw:376 Da) or high (Evan's blue-labelled albumin (EBA), Mw:67 kDa) molecular weight permeability markers, respectively. TEER was measured through an EVOM resistance meter and STX electrodes (World Precision Instruments, Hertfordshire, UK). After TEER readings, the inserts were washed thoroughly with Hank's Balanced Salt Solution (HBSS) and transferred to fresh 12-well plates containing HBSS (2 mL). NaF (10 µg/mL) or EBA (165 µg/mL) was then added to the luminal chambers and samples were removed every 20 min from luminal and abluminal chambers to detect the respective concentrations of dyes by spectrophotometry (EBA, 610 nm) or fluorometry (NaF, 440/525 nm excitation/emission). The flux across the cell-free inserts was determined as previously described (Abdullah and Bayraktutan, 2014).

Measurement of total TNF-α levels

TNF-α levels were detected in cell culture supernatants using the DuoSet ELISA development assay kit (R&D Systems, Abingdon, UK). Briefly, supernatants collected from endothelial cells or astrocytes, subjected to various experimental conditions, were centrifuged at 1000 *g* for 10 min to remove the excess debris. Samples or standards were then added to 96-well plates pre-coated with a capture antibody and incubated at room temperature for 2 h. The plates were then washed with PBS containing Tween-20 (0.05%) and successively incubated with an antibody specific for recombinant human TNF-α for 2 h at room temperature. The plates were then washed and incubated with HRP-linked secondary antibody (1:200) and substrate solution for 20 min in the dark, respectively. After stopping the reactions by sulphuric acid (2 mmol/L), the optical densities were detected by BMG LABTECH Omega plate reader

set to 450 nm with a wavelength correction of 570 nm. The concentration of TNF-α (pg/mL) was calculated using the standard curves.

Measurement of total $O_2^{\cdot -}$ levels and NADPH Oxidase Activity

The levels of total $O_2^{\cdot -}$ and NADPH oxidase activity were determined as previously by cytochrome *C* reduction and lucigenin chemiluminescence assays (Abdullah and Bayraktutan, 2014).

Immunoblotting

Equal amount of total protein samples (50-65 μg) obtained from endothelial cells and were electrophoresed on 10% SDS-PAGE gels before transferring onto polyvinylidene fluoride membrane (GE Healthcare, Buckinghamshire, UK). The membranes were then successively incubated with a combination of primary antibodies specific for β-actin (mouse; cat. no. A5441; internal control; 1:30000; Sigma, Dorset,UK) and claudin-5 (rabbit; cat. no. ab53765; 1:500; Abcam, Cambridge, UK) or occludin (rabbit; cat. no. sc5562; 1:650; Santa Cruz Biotech, Heidelberg, Germany) and infrared dye-conjugated appropriate secondary antibodies (goat anti-mouse; cat. no. 926-68020 and goat anti-rabbit; cat. no. 926-32211; 1:30000; Li-Cor Biosciences, Cambridge, UK). The blots were visualised and analysed using the Li-Cor Odyssey Infrared imaging system (Li-Cor Biosciences).

Gelatin zymography

Equal amounts of culture media used to grow HBMEC or HA (~5 μL) or total cell protein (20-70μg/mL) were run on 10% polyacrylamide gel containing 0.1% gelatin. The gels were then washed in 2.5% Triton X-100 for 30 min before treating overnight with a buffer containing 50 mmol/L Tris (pH 7.5), 10 mmol/L $CaCl_2$, 50 mmol/L NaCl and 0.05% Brij-35 (Merck Millipore, Nottingham, UK). The gels were then stained for 2 h in 0.1% Coomassie Brilliant Blue-G dye containing 25% methanol and 5% acetic acid and destained for a minimum of 1 h in 50% methanol and 25% acetic acid. Bands were scanned and quantified using Li-Cor

Odyssey Infrared imaging system and the readings were normalized to “mg protein”. The amounts of total proteins in the samples were detected by Coomasie Plus assay kit according to manufacturer’s instructions (Thermo Fisher Scientific, UK).

F-actin staining

Cells grown to about 80% confluence on glass coverslips were fixed and permeabilised in 4% paraformaldehyde/PBS and 0.1% Triton X-100/PBS for 15 min, respectively. The coverslips were then blocked for 30 min with 10% BSA/PBS before staining actin filaments in the dark with rhodamine-labelled phalloidin dye (5 U/mL, Invitrogen, Paisley, UK) for ~25 min. Slides were viewed by Zeiss Axio Observer fluorescence microscope.

TUNEL staining

TUNEL staining was performed using the DeadEnd™ colourimetric TUNEL detection kit as per the manufacturer’s instructions (Promega, Southampton, UK). Briefly, cells cultured on coverslips were fixed and permeabilised as above before equilibrating for 10 min with a solution containing potassium cacodylate (200 mmol/L), Tris-HCl (25 mmol/L), dithiothreitol (0.2 mmol/L), BSA (250 mg/L) and cobalt chloride (2.5 mmol/L). To allow end-labelling to occur, the coverslips were then incubated for 60 min with recombinant terminal deoxynucleotidyl transferase (rTdT) reaction mix containing equilibrium buffer (98 µL), biotinylated nucleotide mix (1µL) and rTDT enzyme (1µL). The reaction was terminated by dipping coverslips into 20X SSC buffer prior to blocking and staining them with 0.3% H_2O_2 and horseradish peroxidase-labelled streptavidin (500 mg/L; 1:500), respectively. TUNEL-positive cells were then visualised by diaminobenzidine which gave the dark brown colour to apoptotic cells. Cells were viewed under a light microscope and counted (TUNEL-positive vs total) from 3 different fields per coverslip before calculating the mean values for these areas.

Caspase-3/7 activity

Caspase-3/7 activities were measured by Apo-ONE homogeneous caspase-3/7 assay kit as per manufacturer's instructions (Promega, Southampton, UK). Briefly, cells grown to 95% confluence in 96-well plates were exposed to experimental conditions. To initiate the reaction, 100 μL of media was removed from each well and replaced by 100 μL of caspase 3/7 assay buffer, containing the non-fluorescent caspase substrate, rhodamine 110, bis-(N-CBZL-aspartyl-L-glutamyl-L-valyl-L-aspartic acid amide; Z-DEVD-R110). Plates were then frozen at -80°C overnight. On the following day, the plates were completely thawed on a plate shaker before reading the fluorescence, generated by the caspase-3/7-mediated cleavage of the non-fluorescent caspase substrate to fluorescent rhodamine-110 (excitiation/emission: 485/520 nm). Blanks were subtracted from the readings before normalising activity against "mg protein". Because the assay kit was found to be sensitive to the media employed, two different controls i.e. RPMI lacking FBS, pyruvate as well as glucose and EC media were used in measurements of caspase activity to represent controls for OGD and OGD+R phase, respectively.

Cell Viability Assay

To detect the effects of different treatment regimens on cell viability, an aliquot of cells were mixed with 0.1% Trypan blue for ~4 min before counting 100 cells under a light microscope to work out the % viability rates.

Statistical Analysis

Data are presented as mean±SEM. Statistical analyses were conducted using IBM SPSS statistics 20.0 software package. Mean values were compared by Student's two-tailed *t*-test or one-way ANOVA, where appropriate, followed by Dunnett's post-hoc testing. $P<0.05$ was considered significant.

Results

Effects of OGD±R on TNF-α levels

To assess whether the availability of TNF-α release is augmented by ischaemia-reperfusion (IR) injury in major cell lines associated with the formation and maintenance of BBB, HBMEC and HA were first subjected to the incremental periods of OGD (30 min to 20 h). This revealed a significant increase in both cells within 30 min of challenge that lasted up to 6 h before declining at 12 h but remaining radically higher than controls. It is of note that the level of basal TNF-α release remained largely unaffected in both cell types exposed to normoxic conditions for the indicated periods. It is also noteworthy that the level of TNF-α was considerably higher in endothelial cells compared to astrocytes. Interestingly, reintroduction of oxygen and glucose to the cells (used to mimic reperfusion) evoked further increases in endothelial, but not astrocytic, release of TNF-α (Figure 1A-D).

Effect of TNF-α inhibition on BBB integrity and function

To assess whether TNF-α is involved in OGD±R-mediated BBB damage, a contact co-culture model of human BBB composed of BMEC and astrocytes was exposed to 4 h of OGD alone or followed by reperfusion in the absence or presence of an anti-TNF-α antibody. While OGD±R significantly perturbed barrier integrity and function, neutralisation of TNF-α dramatically improved both parameters as evidenced by marked increases in TEER and concomitant decreases in NaF and EBA flux, respectively thereby proving TNF-α as an instrumental player in (post-)ischaemic barrier damage (Figure 2A-C). 0.2 μg/ml of anti-TNF-α antibody was used during this study due to its efficacy in normalising OGD-induced release of TNF-α in HBMEC (Figure 2D). Exposure of co-cultures to anti-TNF-α antibody alone for 4 or 20 h did not affect paracellular permeability. Interestingly, despite causing further reductions in TNF-α release, application of a higher concentration of anti-TNF-α antibody (0.5 μg/ml) did not further improve barrier integrity and function, indicating that normalisation of this particular cytokine is sufficient to negate its barrier-disruptive effect (Figure 3A-C).

Effect of TNF-α inhibition on NADPH oxidase activity and $O_2^{\cdot-}$ release

The basal levels of NADPH oxidase and $O_2^{\cdot-}$ appeared to be significantly higher (>2-fold) in HBMEC than HA. OGD±R significantly increased NADPH oxidase activity and $O_2^{\cdot-}$ generation in both cells without affecting fold-differences observed at basal levels. Again, negation of TNF-α activity by a specific antibody substantially diminished the effects of OGD±R on oxidase activity and $O_2^{\cdot-}$ release (Figure 4A-D). Exposure of either cell line to anti-TNF-α antibody alone for 4 or 20 h did not have any impact on basal $O_2^{\cdot-}$ release or oxidase activity (Figure 5A-D).

Effect of TNF-α inhibition on MMP activity

OGD±R elevated the level of both intracellular and extracellular (secreted) pro-MMP-2 in HBMEC. Although the expression of intracellular pro-MMP-9 stayed below the level of detection in control cells and those subjected to OGD alone, reperfusion elevated extracellular pro-MMP-9 expression to a level that was detectable by zymography. In contrast, OGD did not alter intracellular and extracellular pro-MMP-2 levels in HA where reperfusion produced a selective increase only in extracellular pro-MMP-2 while pro-MMP-9 could not be detected at all. Inhibition of TNF-α dramatically suppressed all the aforementioned increases (Figure 6A-C). It is of note here that no pro-MMP-2 or pro-MMP-9 expressions were detected in serum only samples. Again, exposure of either cell line to anti-TNF-α antibody alone for 4 or 20 h did not affect basal intracellular or secreted pro-MMP-2 levels (Figure 7A-B).

Effects of TNF-α inhibition on tight junction protein expression and cytoskeleton

OGD produced significant decreases in claudin-5 and occludin protein expressions which were further reduced by reperfusion in case of claudin-5. Neutralisation of TNF-α attenuated the effects of OGD±R on claudin-5 protein expression while normalising that of occludin. Treatments with anti-TNF-α antibody alone did not affect either protein expression (Figure 8A-D).

In concert with these changes, OGD±R evoked dramatic changes in cellular architecture as evidenced by formation of actin stress fibres in both HBMEC and HA. While inhibition of TNF-α effectively negated OGD±R-evoked stress fibre formation, it had no affect effect on cytoskeleton in normal settings (Figure 9A-B).

Effect of TNF-α inhibition on BBB-related cell apoptosis

OGD and OGD+R significantly elevated the number of apoptotic nuclei (arrows) in HBMEC and HA where the addition of an anti-TNF-α antibody effectively suppressed the rates of DNA fragmentation. Changes in pro-apoptotic caspase-3/7 enzyme activities in HBMEC and HA were reflective of those seen in TUNEL stainings. The magnitude of increases in these particular enzyme activities was radically greater in HBMEC. Co-treatment of cells with the anti-TNF-α antibody substantially suppressed the deleterious effects of ischaemic injury, implying that OGD±R modulates the activity of these apoptotic enzymes through TNF-α. It is of note that treatment with TNF-α antibody was more influential in HA. Two different types of controls had to be used in these experiments due to sensitivity of the kit used for media. Hence, control RPMI that lacked FBS, pyruvate and glucose served as control for 4 h OGD±anti-TNF-α antibody experiments while control ECM that possessed these served as control for 4 h OGD+R±anti-TNF-α antibody experiments. To reveal the actual difference in enzyme activity, the control readings were subtracted from the respective experimental readings prior to graphical illustration. Treatments with anti-TNF-α antibody did not affect basal caspase-3/7 activities in either cell line (Figures 10A-C and 11A-C).

Discussion

Brain oedema stemming from disruption of the BBB constitutes the leading cause of mortality within the first week after an ischaemic stroke. Accumulating evidence demonstrate that acute inflammatory reactions accompanied by exaggerated release of pro-inflammatory cytokines significantly contribute to the initiation and progression of this phenomenon

(Ferrarese et al., 1999; Hosomi et al., 2005; Yang et al., 1999). Spurred on by our recent study exhibiting an intimate correlation between the enhanced availability of TNF-α and the BBB damage, this study sought to reveal whether neutralisation of TNF-α may be of therapeutic value in attenuating the deleterious effects of IR injury on cerebral barrier (Abdullah and Bayraktutan, 2014). Given that TNF-α is intricately involved in the pathogenesis of several neurological conditions, elucidation of this particular point may have far greater implications than those are presently anticipated (Hasturk et al., 2009; Pan et al., 2006; Zaremba et al., 2001). As cerebrovascular activity gradually deteriorates after a cerebral attack, we primarily investigated the time course of IR-mediated TNF-α release in the most important cellular components of the BBB, i.e. BMEC and astrocytes, which revealed a biphasic pattern in both cells subjected to increasing periods of OGD (0.5-20 h) alone or followed by reperfusion (20 h). Although remained significantly higher than the respective controls at all the time points studied, the initial peak observed in TNF-α secretion at 0.5 h of insult lasted up to 6 h before dipping slightly but markedly at 12 h. Considering the substantially higher levels of TNF-α in normal and IR-induced BMEC versus the corresponding astrocytes (by ≥2.5-fold), it is safe to suggest that endothelium, but not astrocyte endfeet, constitutes the main vascular locus that regulates cerebral homeostasis by synthesising and/or releasing a wide range of vasoactive agents including bradykinin, nitric oxide and various cytokines (Abdullah and Bayraktutan, 2014; Bayraktutan, 2002). Indeed, reperfusion-mediated selective potentiation of TNF-α release in BMEC alone confirms endothelial dysfunction as a salient phenomenon in IR-evoked neurovascular damage (Ferrarese et al., 1999; Hasturk et al., 2009; Yang et al., 1999) while simultaneously indicating that astrocytes are better equipped to cope with the deleterious effects of ischaemic injury and ensuing secondary complications like inflammation (Bresgen et al., 2006; Chen and Swanson, 2003).

Having ascertained the pattern of TNF-α release in BBB-related cells, all subsequent experiments were performed using a clinically-relevant period of OGD (4 h) alone or followed by reperfusion (20 h). First, using a co-culture model of human BBB comprising HBMEC and HA, this study has verified that OGD significantly compromises barrier integrity and function as evidenced by dramatic decreases in TEER and concurrent increases in paracellular flux of NaF (376 Da) and EBA (67 kDa), respectively (Gibson et al., 2014; Rakkar et al., 2014). As expected, reperfusion further augmented the extent of OGD-evoked barrier damage. Detection of relatively lower quantities of EBA across the *in vitro* barrier signified that the size of some BBB openings were not big enough to allow the passage of bigger substances. Inhibition of TNF-α by a neutralising antibody radically attenuated, but not neutralised, the deleterious effects of OGD±R on barrier integrity and function similar to some previous studies reporting a considerable improvement in neurological outcome and concurrent reductions in haemorrhage, infarct size and cell death after ischaemia (Barone et al., 1997; Yang et al., 1999; Yang et al., 1998; Yenari et al., 2006). Taken together these findings imply the putative contributions of other mechanisms and possibly cytokines to IR-mediated neurovascular damage.

Oxidative stress, characterised by an increased presence of reactive oxygen species, especially $O_2^{\cdot -}$, represents one such mechanisms. A recent study examining the specific causes of TNF-α-induced BBB damage has in part ascribed this defect to the activation of NADPH oxidase and consequent production of $O_2^{\cdot -}$ in BMEC and astrocytes. Although levels of both increases were dictated by the duration of incubation (2-24 h, peaking at 6 h), they appeared to be independent of the concentration of TNF-α tested (5-20 ng/ml), indicating the inability of TNF-α to exert further barrier damage beyond a certain threshold (Abdullah and Bayraktutan, 2014). Considering the abundant release of TNF-α during the first 6 h of ischaemic insult, it is inevitable that oxidative stress plays a central role in the early phases of ischaemic stroke.

Indeed, OGD±R-mediated increases in both endothelial and astrocytic NADPH oxidase activity and $O_2^{\cdot -}$ production corroborated this assumption. Similar to previous studies, the level of increases induced by reperfusion in oxidase activity and $O_2^{\cdot -}$ production appeared to be small but significant in both cell types (Abdullah and Bayraktutan, 2014; Gibson et al., 2014). Here, measurement of significantly greater levels of oxidase activity and $O_2^{\cdot -}$ in BMEC has reinforced the decisive role of endothelial dysfunction in vasculopathies while discovery of substantially diminished oxidase activity in astrocytes has provided an additional explanation for their resistance to oxidative stress which had previously been attributed to the existence of strong inherent antioxidant capacity in them (Abdullah and Bayraktutan, 2014; Bresgen et al., 2006; Chen and Swanson, 2003). NADPH oxidase is regarded as the main source of $O_2^{\cdot -}$ in BBB-related cells, neurons, leukocytes and post-ischaemic brain. Suppression of its activity by structurally distinct inhibitors like DPI and apocynin as well as knockout of its membrane-bound or cytosolic subunits e.g. gp91-phox and p47-phox in mice has been coupled to the effective maintenance of barrier integrity and neuronal viability following an ischaemic episode (Abdullah and Bayraktutan, 2014; Rakkar et al., 2014; Suh et al., 2007). In the current study, inhibition of oxidase activity and $O_2^{\cdot -}$ generation in BMEC and astrocytes by a TNF-α IgG demonstrates that NADPH oxidase acts downstream to TNF-α in ischaemic settings and is manipulated by it to disrupt BBB. Manipulation of this particular oxidase by another inflammatory cytokine i.e. IL-1β has also been reported in pial arteries of a stroke model where the enhanced release of bradykinin during cerebral ischaemia caused an increase in IL-1β levels which in turn activated NADPH oxidase to perturb BBB (Woodfin et al., 2011).

Activation of MMPs that digest various components of the basement membrane, notably collagen IV, laminin and fibronectin may also contribute to OGD±R/TNF-α pathway-evoked cerebral barrier disruption. To date, many members of MMP family of endopeptidases sharing similar primary structure and requiring Zn^{+2} for their catalytic activity have been identified.

Amongst these, MMP-2, MMP-9 and their inactive proforms represent the most studied isoforms that have closer relevance to ischaemic cerebral injury (Nagase et al., 1997; del Zoppo et al., 2007). Since active forms of MMP-2 and MMP-9 are considerably less stable than their inactive proforms and isolation, handling and the type of cells significantly affect their detection in active form (Fujimura et al., 1999; Romanic et al., 1998) , the levels of pro-MMPs were studied in the present study which revealed substantial increases in intracellular and extracellular levels of endothelial pro-MMP-2, suggesting the potential involvement of its active form in OGD±R/TNF-α pathway-evoked cerebral barrier disruption. Although a similar increase was also recorded in astrocytes, this appeared to be confined to the extracellular isoform during the reperfusion phase. In contrast, despite selectively detecting extracellular pro-MMP-9 in BMEC during reperfusion phase, neither active nor pro-MMP-9 could be detected in astrocytes. Collectively, these data show endothelium as the main source of MMPs in ischaemic conditions and add weight to the notion that astrocytes can only generate pro-MMP-9 under certain experimental conditions (Massengale et al., 2002). Similarly, several previous studies have also attributed increases in infarct volume, BBB permeability and haemorrhagic transformation to ischaemic injury-mediated overexpression of (pro)-MMP-2/9 (Bauer et al., 2010; Fujimura et al., 1999; Romanic et al., 1998; Heo et al., 1999). Normalisation or attenuation of pro-MMP-2 (and where detectable pro-MMP-9) levels by an anti-TNF-α antibody during OGD and OGD+R, respectively indicate that neutralisation of TNF-α exerts better protection during the early stages of ischaemic injury while other elements become more prominent during the later phases of injury. Indeed, normalisation of MMP activities by apocynin and DPI in BMEC exposed to TNF-α (5 ng/ml) propose NADPH oxidase and $O_2^{\cdot -}$ as important regulators of MMP activity. However, reduction in basal lamina protein loss resulting from the successive suppression of TNF-α and MMP-9 activity was important in

restoring BBB integrity and function in rodents subjected to peripheral thermal injury (Reyes et al., 2009).

In addition to enzymatic digestion of basement membrane components, the changes in cellular architecture may also accentuate the permeability of cerebral barrier. Experiments focusing on the potential structural alterations in microfilaments, a pivotal component of cytoskeleton, revealed that both BMEC and astrocytes cultured in normal conditions displayed a cortical actin distribution which facilitates the formation of junctional complexes by anchoring integral membrane proteins occludin and claudin-5 with the membrane-associated proteins ZO-1 and ZO-2 to prevent paracellular flux. In contrast, cells exposed to OGD±R underwent a moderate shrinkage and developed thick stress fibres that traversed the cells and produced a tensile centripetal force to pull junctional proteins inwards to create intercellular openings. Besides maintaining appropriate cytoskeletal structure, actin also regulates the growth; Ca^{2+} uptake, release and signaling; Cl^{-} conductance and glutamate uptake in astrocytes (Cotrina et al., 1998; Zigmond., 1996; Duan et al., 1999; Sergeeva et al., 2000). Considering the pivotal roles played by astrocytes to maintain physiological pH in the extracellular space, supply neurons with nutrients, remove metabolic byproducts and regulate synaptic development and strength (Nedergaard et al., 2003; Haydon., 2001), it is safe to suggest that ischaemia-induced neuroinflammation and ensuing actin filament reorganisation may elicit astrocyte and BBB dysfunction. Indeed, recent studies coupling reorganisation of microfilaments in astrocyte networks to significant alterations in Ca^{2+} signalling systems, Na^{+}/K^{+}-ATPase and glutamate transporters and those showing increased release of pro-inflammatory cytokines in a model of lipopolysaccharide-induced neuroinflammation fully support this notion (reviewed by Hansson., 2015).

Other than dislocating TJ proteins, OGD±R also caused significant reductions in TJ protein expressions. While both OGD and OGD+R diminished occludin levels in equal measures, the

decrease in claudin-5 levels appeared to be more prominent after the onset of reperfusion. Similar decreases in these protein levels were also reported in experimental stroke models (Liu et al., 2012; McColl et al., 2008; Yang et al., 2006). As the injection of TNF-α caused significant reductions in occludin and claudin-1 mRNA and protein levels in the intestines of a mouse model of fulminant hepatic failure and inhibition of TNF-α decreased intestinal permeability by stemming claudin-1 and occludin downregulation (Li et al., 2012), we assessed the impact of a TNF-α neutralising antibody on cytoskeletal organization and TJ protein expressions. In concert with its effects on the BBB permeability, the inhibition of TNF-α maintained normal endothelial cell and astrocyte morphology by reducing IR-evoked stress fibre formation while significantly improving (claudin-5) or normalising (occludin) TJ protein expressions.

Increasing evidence report that apoptosis of BMEC and astrocytes exacerbates the extent of ischaemic injury by compromising the formation of TJs and microvascular integrity through a range of mechanisms including elevated availability of ROS, Bax protein overexpression, mitochondrial dysfunction and upregulation of caspase-3 and other caspase family members (Giffard and Swanson, 2005; Kontos, 2001; Krupinski et al., 2000; Scarabelli et al., 2002). However, since little is known about the exact molecular mechanism of apoptosis in vascular tissue after IR, the present study investigated the impact of OGD±R on HBMEC and HA apoptosis and searched whether TNF-α is involved in this phenomenon. Consequently, it has been shown that OGD±R significantly increases pro-apoptotic caspase-3/7 activities and DNA fragmentation rates in both BMEC and astrocytes. Although detection of higher rates of apoptosis after reperfusion suggests the idea that oxidative stress contributes to this defect, anti-TNF-α antibody-induced substantial decreases in both parameters proved this particular cytokine as a crucial regulator of vascular cell death after OGD±R.

In conclusion, the current results reveal that exaggerated release of TNF-α during IR injury promotes cerebrovascular damage through concurrent regulations of oxidative stress, MMP activity and BBB-related cell apoptosis. Effective attenuations of these parameters by a TNF-α antibody coupled with improvements in BBB integrity and function strongly suggest that targeting of TNF-α may be of therapeutic value after an ischaemic stroke.

Disclosures

The authors have no financial conflicts of interest.

Sources of funding

This study was supported by a PhD studentship grant to Dr Bayraktutan.

Abbreviations

TNF-α, tumour necrosis factor-alpha; BBB, blood-brain barrier; HBMEC, human brain microvascular endothelial cells; HA, human astrocytes; NaF, sodium fluorescein; EBA, Evan's blue-labelled albumin; TEER, transendothelial electrical resistance; FBS, foetal bovine serum; PBS, phosphate-buffered saline; HBSS, Hank's Balanced Salt Solution; MMP, matrix metalloproteinase; DPI, diphenyleneiodonium; TJs, tight junctions, OGD, oxygen-glucose deprivation; OGD±R, oxygen-glucose deprivation±reperfusion.

References

Abdullah, Z., Bayraktutan, U., 2014. NADPH oxidase mediates TNF-alpha-evoked *in vitro* brain barrier dysfunction: roles of apoptosis and time. Mol. Cell. Neurosci. 61, 72-84.

Allen, C., Srivastava, K., Bayraktutan, U., 2010. Small GTPase RhoA and Its Effector Rho Kinase Mediate Oxygen Glucose Deprivation-Evoked In Vitro Cerebral Barrier Dysfunction. Stroke.

Allen, C.L., Bayraktutan, U., 2009. Antioxidants attenuate hyperglycaemia-mediated brain endothelial cell dysfunction and blood–brain barrier hyperpermeability. Diabetes, Obes. Metab. 11, 480-490.

Ballabh, P., Braun, A., Nedergaard, M., 2004. The blood-brain barrier: an overview: Structure, regulation, and clinical implications. Neurobiol. Dis. 16, 1-13.

Barone, F.C., Arvin, B., White, R.F., Miller, A., Webb, C.L., Willette, R.N., Lysko, P.G., Feuerstein, G.Z., 1997. Tumor Necrosis Factor-α : A Mediator of Focal Ischemic Brain Injury. Stroke 28, 1233-1244.

Basuroy, S., Bhattacharya, S., Tcheranova, D., Qu, Y., Regan, R.F., Leffler, C.W., Parfenova, H., 2006. HO-2 provides endogenous protection against oxidative stress and apoptosis caused by TNF-α in cerebral vascular endothelial cells. Am. J. of Physiol. Cell Physiol. 291, C897-C908.

Bauer, A.T., Burgers, H.F., Rabie, T., Marti, H.H., 2010. Matrix metalloproteinase-9 mediates hypoxia-induced vascular leakage in the brain via tight junction rearrangement. J. Cereb. Blood Flow Metab. 30, 837-848.

Bayraktutan, U., 2002. Free radicals, diabetes and endothelial dysfunction. Diabetes, Obes. Metab. 4, 224-238.

Bresgen, N., Jaksch, H., Bauer, H.-C., Eckl, P., Krizbai, I., Tempfer, H., 2006. Astrocytes are more resistant than cerebral endothelial cells toward geno- and cytotoxicity mediated by short-term oxidative stress. J. Neurosci. Research 84, 1821-1828.

Candelario-Jalil, E., Yang, Y., Rosenberg, G.A., 2009. Diverse roles of matrix metalloproteinases and tissue inhibitors of metalloproteinases in neuroinflammation and cerebral ischemia. Neuroscience 158, 983-994.

Chen, H., Kim, G.S., Okami, N., Narasimhan, P., Chan, P.H., 2011. NADPH oxidase is involved in post-ischemic brain inflammation. Neurobiol. Dis. 42, 341-348.

Chen, H., Song, Y.S., Chan, P.H., 2009. Inhibition of NADPH oxidase is neuroprotective after ischemia-reperfusion. J Cereb Blood Flow Metab 29, 1262-1272.

Chen, Y., Swanson, R.A., 2003. Astrocytes and Brain Injury. J. Cereb. Blood Flow Metab. 23, 137-149.

Cotrina, M.L., Lin, J.H., Nedergaard, M,. 1998. Cytoskeletal assembly and ATP release regulate astrocytic calcium signaling. J. Neurosci. 18, 8794-8804.

Dejana, E., 2004. Endothelial cell-cell junctions: happy together. Nat. Rev. Mol. Cell Biol. 5, 261-270.

Del Zoppo, G.J., Milner, R., Mabuchi, T., Hung, S., Wang, X., Berg, G.I., Koziol, J.A., 2007. Microglial activation and matrix protease generation during focal cerebral ischemia. Stroke. 38, 446-451.

Duan, S., Anderson, C.M., Stein, B.A., Swanson, R.A., 1999. Glutamate induces rapid upregulation of astrocyte glutamate transport and cell-surface expression of GLAST. J. Neurosci. 19, 10193-10200.

Farrall, A.J., Wardlaw, J.M., 2009. Blood–brain barrier: Ageing and microvascular disease – systematic review and meta-analysis. Neurobiol. aging 30, 337-352.

Ferrarese, C., Mascarucci, P., Zoia, C., Cavarretta, R., Frigo, M., Begni, B., Sarinella, F., Frattola, L., De Simoni, M.G., 1999. Increased Cytokine Release From Peripheral Blood Cells After Acute Stroke. J. Cereb. Blood Flow Metab. 19, 1004-1009.

Fujimura, M., Gasche, Y., Morita-Fujimura, Y., Massengale, J., Kawase, M., Chan, P.H., 1999. Early appearance of activated matrix metalloproteinase-9 and blood-brain barrier disruption in mice after focal cerebral ischemia and reperfusion. Brain Res. 842, 92-100.

Gao, X., Zhang, H., Belmadani, S., Wu, J., Xu, X., Elford, H., Potter, B.J., Zhang, C., 2008. Role of TNF-α-induced reactive oxygen species in endothelial dysfunction during reperfusion injury. American Journal of Physiology-Heart Circ. Physiol. 295, H2242-H2249.

Gibson, C.L., Srivastava, K., Sprigg, N., Bath, P.M.W., Bayraktutan, U., 2014. Inhibition of Rho-kinase protects cerebral barrier from ischaemia-evoked injury through modulations of endothelial cell oxidative stress and tight junctions. J. Neurochem.129, 816-826.

Giffard, R.G., Swanson, R.A., 2005. Ischemia-induced programmed cell death in astrocytes. Glia 50, 299-306.
Gu, X., Zhang, J., Brann, D.W., Yu, F.S.X., 2003. Brain and Retinal Vascular Endothelial Cells with Extended Life Span Established by Ectopic Expression of Telomerase. Invest. Ophthalmol. Vis. Sci. 44, 3219-3225.
Hansson, E., 2015, Actin Filament Reorganization in Astrocyte Networks is a Key Functional Step in Neuroinflammation Resulting in Persistent Pain: Novel Findings on Network Restoration. Neurochem. Res. 40, 372-379.
Hasturk, A., Atalay, B., Calisaneller, T., Ozdemir, O., Oruckaptan, H., Altinors, N., 2009. Analysis of Serum Pro-Inflammatory Cytokine Levels after Rat Spinal Cord Ischemia/Reperfusion Injury and Correlation with Tissue Damage. Turk. Neurosurg. 19, 353-359.
Hayashi, K., Nakao, S., Nakaoke, R., Nakagawa, S., Kitagawa, N., Niwa, M., 2004. Effects of hypoxia on endothelial/pericytic co-culture model of the blood-brain barrier. Regul. Peptides 123, 77-83.
Haydon, P.G., 2001, Glia: listening and talking to the synapse. Nat. Rev. Neurosci. 2, 185-193.
Heo, J.H., Lucero, J., Abumiya, T., Koziol, J.A., Copeland, B.R., del Zoppo, G.J. 1999. Matrix metalloproteinases increase very early during experimental focal cerebral ischemia. J. Cereb. Blood Flow Metab. 19, 624-633.
Hosomi, N., Ban, C.R., Naya, T., Takahashi, T., Guo, P., Song, X.y.R., Kohno, M., 2005. Tumor necrosis factor-[alpha] neutralization reduced cerebral edema through inhibition of matrix metalloproteinase production after transient focal cerebral ischemia. J. Cereb. Blood Flow Metab. 25, 959-967.
Hurwitz, A.A., Berman, J.W., Rashbaum, W.K., Lyman, W.D., 1993. Human fetal astrocytes induce the expression of blood-brain barrier specific proteins by autologous endothelial cells. Brain Res. 625, 238-243.
Kahles, T., Luedike, P., Endres, M., Galla, H.J., Steinmetz, H., Busse, R., Neumann-Haefelin, T., Brandes, R.P., 2007. NADPH Oxidase Plays a Central Role in Blood-Brain Barrier Damage in Experimental Stroke. Stroke 38, 3000-3006.
Kim, J.A., Tran, N.D., Wang, S.-J., Fisher, M.J., 2003. Astrocyte regulation of human brain capillary endothelial fibrinolysis. Thromb. Res. 112, 159-165.
Kontos, H.A., 2001. Oxygen Radicals in Cerebral Ischemia: The 2001 Willis Lecture. Stroke 32, 2712-2716.
Krupinski, J., Lopez, E., Marti, E., Ferrer, I., 2000. Expression of Caspases and Their Substrates in the Rat Model of Focal Cerebral Ischemia. Neurobiol. Dis. 7, 332-342.
Li, G.Z., Wang, Z.H., Cui, W., Fu, J.L., Wang, Y.R., Li, U.P., 2012. Tumor necrosis factor alpha increases intestinal permeability in mice with fulminant hepatic failure. World J. Gastroenterol. 18, 5042-5050.
Liu, J., Jin, X., Liu, K.J., Liu, W., 2012. Matrix Metalloproteinase-2-Mediated Occludin Degradation and Caveolin-1-Mediated Claudin-5 Redistribution Contribute to Blood-Brain Barrier Damage in Early Ischemic Stroke Stage. J. Neurosci. 32, 3044-3057.
Massengale, J.L., Gasche, Y., Chan, P.H., 2002. Carbohydrate source influences gelatinase production by mouse astrocytes in vitro. Glia. 38, 240-245.
McColl, B.W., Rothwell, N.J., Allan, S.M., 2008. Systemic Inflammation Alters the Kinetics of Cerebrovascular Tight Junction Disruption after Experimental Stroke in Mice. J. Neurosci. 28, 9451-9462.
Nagase, H., 1997. Activation mechanisms of matrix metalloproteinases. Biol. Chem. 378, 151-160.

Nedergaard, M., Ransom, B., Goldman, S.A., 2003, New roles for astrocytes: redefining the functional architecture of the brain. Trends. Neurosci. 26, 523-530.
Pan, W., Ding, Y., Yu, Y., Ohtaki, H., Nakamachi, T., Kastin, A.J., 2006. Stroke upregulates TNF-alpha transport across the blood-brain barrier. Exp. Neurol. 198, 222-233.
Parks, W.C., Wilson, C.L., Lopez-Boado, Y.S., 2004. Matrix metalloproteinases as modulators of inflammation and innate immunity. Nat. Rev. Immunol. 4, 617-629.
Rakkar, K., Srivastava, K., Bayraktutan, U., 2014. Attenuation of urokinase activity during experimental ischaemia protects the cerebral barrier from damage through regulation of matrix metalloproteinase-2 and NAD(P)H oxidase. Eur. J. Neurosci. 39, 2119-2128.
Reyes, R., Guo, M., Swann, K., Shetgeri, S.U., Sprague, S.M., Jimenez, D.F., Barone, C.M., Ding, Y., 2009. Role of tumor necrosis factor- α and matrix metalloproteinase-9 in blood-brain barrier disruption after peripheral thermal injury in rats. J. Neurosurg. 110, 1218-1226.
Romanic, A.M., White, R.F., Arleth, A.J., Ohlstein, E.H., Barone, F.C., 1998. Matrix Metalloproteinase Expression Increases After Cerebral Focal Ischemia in Rats: Inhibition of Matrix Metalloproteinase-9 Reduces Infarct Size. Stroke 29, 1020-1030.
Rosenberg, G.A., Estrada, E.Y., Dencoff, J.E., Hsu, C.Y., 1998. Matrix Metalloproteinases and TIMPs Are Associated With Blood-Brain Barrier Opening After Reperfusion in Rat Brain. Editorial Comment. Stroke 29, 2189-2195.
Sandoval, K.E., Witt, K.A., 2008. Blood-brain barrier tight junction permeability and ischemic stroke. Neurobiol. Dis. 32, 200-219.
Scarabelli, T.M., Stephanou, A., Pasini, E., Comini, L., Raddino, R., Knight, R.A., Latchman, D.S., 2002. Different Signaling Pathways Induce Apoptosis in Endothelial Cells and Cardiac Myocytes During Ischemia/Reperfusion Injury. Circ. Res. 90, 745-748.
Sergeeva, M., Ubl, J.J., Reiser, G., 2000. Disruption of actin cytoskeleton in cultured rat astrocytes suppresses ATP- and bradykinin-induced [Ca(2+)](i) oscillations by reducing the coupling efficiency between Ca(2+) release, capacitative Ca(2+) entry, and store refilling. Neuroscience 97, 765-769.
Shao, B., Bayraktutan, U., 2013. Hyperglycaemia promotes cerebral barrier dysfunction through activation of protein kinase C-β. Diabetes, Obes. Metab. 15, 993-999.
Srivastava, K., Shao, B., Bayraktutan, U., 2013. PKC-beta exacerbates in vitro brain barrier damage in hyperglycemic settings via regulation of RhoA/Rho-kinase/MLC2 pathway. J. Cereb. Blood Flow Metab.33(12),1928-36.
Suh, S.W., Gum, E.T., Hamby, A.M., Chan, P.H., Swanson, R.A., 2007. Hypoglycemic neuronal death is triggered by glucose reperfusion and activation of neuronal NADPH oxidase. J. Clin. Invest. 117, 910-918.
Williams, R., Yao, H., Peng, F., Yang, Y., Bethel-Brown, C., Buch, S., 2010. Cooperative induction of CXCL10 involves NADPH oxidase: Implications for HIV dementia. Glia 58, 611-621.
Woodfin, A., Hu, D.-E., Sarker, M., Kurokawa, T., Fraser, P., 2011. Acute NADPH oxidase activation potentiates cerebrovascular permeability response to bradykinin in ischemia-reperfusion. Free Radical Biol. Med. 50, 518-524.
Yang, G.-Y., Gong, C., Qin, Z., Liu, X.-H., Lorris Betz, A., 1999. Tumor necrosis factor alpha expression produces increased blood-brain barrier permeability following temporary focal cerebral ischemia in mice. Mol. Brain Res. 69, 135-143.
Yang, G.-Y., Gong, C., Qin, Z., Ye, W., Mao, Y., Bertz, A.L., 1998. Inhibition of TNFα attenuates infarct volume and ICAM-1 expression in ischemic mouse brain. NeuroReport. 9, 2131-2134.
Yang, Y., Estrada, E.Y., Thompson, J.F., Liu, W., Rosenberg, G.A., 2006. Matrix metalloproteinase-mediated disruption of tight junction proteins in cerebral vessels is

reversed by synthetic matrix metalloproteinase inhibitor in focal ischemia in rat. J. Cereb. Blood Flow Metab. 27, 697-709.
Yenari, M.A., Xu, L., Tang, X.N., Qiao, Y., Giffard, R.G., 2006. Microglia Potentiate Damage to Blood-Brain Barrier Constituents: Improvement by Minocycline In Vivo and In Vitro. Stroke 37, 1087-1093.
Zaremba, J., Skrobanski, P., Losy, J., 2001. Tumour necrosis factor-alpha is increased in the cerebrospinal fluid and serum of ischaemic stroke patients and correlates with the volume of evolving brain infarct. Biomed. Pharmacother. 55, 258-263.
Zhang, C., Xu, X., Potter, B.J., Wang, W., Kuo, L., Michael, L., Bagby, G.J., Chilian, W.M., 2006. TNF-alpha Contributes to Endothelial Dysfunction in Ischemia/Reperfusion Injury. Arterioscler. Thromb. Vasc. Biol. 26, 475-480.
Zigmond, S.H., 1996. Signal transduction and actin filament organization. Curr. Opin. Cell Biol. 8, 66-73.

Figure Legends

Figure 1. The effects of OGD±R on TNF-α levels. HBMEC and HA were exposed to OGD alone for a period of 30 min, 1, 2, 4, 6, 12 and 20 h or followed by 20 h of reperfusion. Both OGD and OGD+R significantly increased TNF-α levels in both HBMEC **(A, C)** and HA **(B, D)** as early as 30 min lasting up to 20 h compared with untreated groups. Data are expressed as mean±SEM from 10 different experiments. $^{*}p<0.05$ vs control, $^{\dagger}p<0.05$ vs 30 min treatment group, $^{\#}p<0.05$ vs 1 h treatment group.

Figure 2. The effects of OGD±R on BBB integrity and function. HBMEC-HA co-cultures were exposed to 4 h of OGD alone or followed by 20 h of reperfusion (OGD+R) in the absence or presence of an inhibitor for TNF-α, an anti-TNF-α antibody. While OGD±R significantly impaired BBB integrity and function, co-treatments with TNF-α antibody attenuated their impact on BBB integrity **(A)** as well as NaF **(B)** and EBA **(C)** flux. Data are expressed as mean±SEM from 8 different experiments. $^{*}p<0.05$ vs control, $^{\dagger}p<0.05$ vs OGD, $^{\#}p<0.05$ vs OGD+anti-TNF-α antibody, $^{\ddagger}p<0.05$ vs OGD+R.

Figure 3. The effect TNF-α inhibition on BBB integrity and function. Exposure of HBMEC-HA co-cultures to two different concentrations of an anti-TNF-α antibody alone for 4 and/or 20 h had no effect on BBB integrity **(A)** as well as NaF **(B)** and EBA **(C)** flux. Data are expressed as mean±SEM from 6 different experiments.

Figure 4. The effects of OGD±R on total $O_2^{\cdot-}$ production and NADPH oxidase activity. HBMEC and HA were exposed to 4 h of OGD alone or followed by 20 h of reperfusion (OGD+R) in the absence or presence of an anti-TNF-α antibody. Compared to controls, both OGD and OGD+R enhanced $O_2^{\cdot-}$ release and NADPH oxidase activity in HBMEC **(A, C)** and HA **(B, D)** that were markedly reduced by treatments with an anti-TNF-α antibody. Data are expressed as mean±SEM from 12 different experiments. $^{*}p<0.05$ vs control, $^{\dagger}p<0.05$ vs OGD, $^{\#}p<0.05$ vs OGD+anti-TNF-α antibody, $^{\ddagger}p<0.05$ vs OGD+R.

Figure 5. The effect TNF-α inhibition on total $O_2^{\cdot-}$ production and NADPH oxidase activity. Incubations with anti-TNF-α antibody (0.2 μg/ml) alone for 4 or 20 h did not alter $O_2^{\cdot-}$ production and NADPH oxidase activity in HBMEC **(A, C)** or HA **(B, D)**. Data are expressed as mean±SEM from 4 different experiments.

Figure 6. The effects of OGD±R on MMP activities. Representative gelatin zymographies showing the impact of 4 h of OGD alone or followed by 20 h of reperfusion (OGD+R) in the absence or presence of an anti-TNF-α antibody on MMP-2 and MMP-9 activities in HBMEC

(A, C) and HA **(B)**. OGD±R caused significant increases in intracellular and extracellular MMP-2 activity in HBMEC while an increase is only detected in extracellular MMP-2 during reperfusion phase in HA. OGD+R but not OGD alone caused a significant increase in extracellular MMP-9 in HBMEC. Treatments with TNF-α antibody reduced all the observed increases in MMP-2 and MMP-9 activities. Data are expressed as mean±SEM from 7 different experiments. $^{*}p<0.05$ vs control, $^{\dagger}p<0.05$ vs OGD, $^{\#}p<0.05$ vs OGD+anti-TNF-α antibody, $^{\ddagger}p<0.05$ vs OGD+R.

Figure 7. The effect TNF-α inhibition on MMP activities. Treatment with an anti-TNF-α antibody (0.2 μg/ml) alone for 4 or 20 h did not affect intracellular or secreted pro-MMP-2 expression in HBMEC **(A)** and HA **(B)**. Data are expressed as mean±SEM from 4 different experiments.

Figure 8. The effects of OGD±R and TNF-α inhibition on TJ protein expressions. Representative Western blots and densitometric analyses of claudin-5 **(A)** and occludin **(B)** in HBMEC subjected to 4 h of OGD alone or followed by 20 h of reperfusion (OGD+R) in the absence and presence of an anti-TNF-α antibody. OGD±R caused significant reductions in both claudin-5 and occludin protein levels in HBMEC where inhibition of TNF-α antibody attenuated the level of decreases. Treatment with an anti-TNF-α antibody (0.2 μg/ml) alone for 4 or 20 h had no effect on either protein expression **(C, D)**. Data are expressed as mean±SEM from ≥4 different experiments. $^{*}p<0.05$ vs control, $^{\dagger}p<0.05$ vs OGD, $^{\#}p<0.05$ vs OGD+anti-TNF-α antibody, $^{\ddagger}p<0.05$ vs OGD+R.

Figure 9. The effects of OGD±R and TNF-α inhibition on cytoskeletal organisation. F-actin staining revealing cytoskeletal formation was performed with rhodamine-labelled phalloidin dye in HBMEC **(A)** and HA **(B)** subjected to an anti-TNF-α antibody (0.2 μg/ml) alone or OGD±R in the absence and presence of an inhibitor for TNF-α. OGD±R induced actin stress fibres formation in both cells (indicated by arrows) which were attenuated by anti-TNF-α

antibody. Treatment with the anti-TNF-α antibody alone for 4 or 20 h did not influence actin filament formation. Scale bars = 20μm. Data are expressed as mean±SEM from 8 different experiments.

Figure 10. The effects of OGD±R and TNF-α inhibition on apoptosis and caspase-3/7 activity in HBMEC. 4 h of OGD alone or followed by 20 h of reperfusion (OGD+R) increased DNA fragmentation rates, an indicator of apoptosis **(A)** and caspase-3/7 activities **(B)**. Inhibition of TNF-α by an antibody attenuated OGD±R-evoked changes in both parameters without affecting their basal levels **(C)**. Representative TUNEL staining showing apoptotic cells indicated by arrows in HBMEC Scale bars = 20μm. Data are expressed as mean±SEM from 8 different experiments. $^{*}p<0.05$ vs OGD, $^{\dagger}p<0.05$ vs OGD+R.

Figure 11. The effects of OGD±R and TNF-α inhibition on apoptosis and caspase-3/7 activity in HA. 4 h of OGD alone or followed by 20 h of reperfusion (OGD+R) increased DNA fragmentation rates, an indicator of apoptosis **(A)** and caspase-3/7 activities **(B)**. Inhibition of TNF-α by an antibody attenuated OGD±R-evoked changes in both parameters without affecting their basal levels **(C)**. Representative TUNEL staining showing apoptotic cells indicated by arrows in HBMEC Scale bars = 20μm. Data are expressed as mean±SEM from 8 different experiments. $^{*}p<0.05$ vs OGD, $^{\dagger}p<0.05$ vs OGD+R.

Figure 1
See separate sheet

Figure 2
A

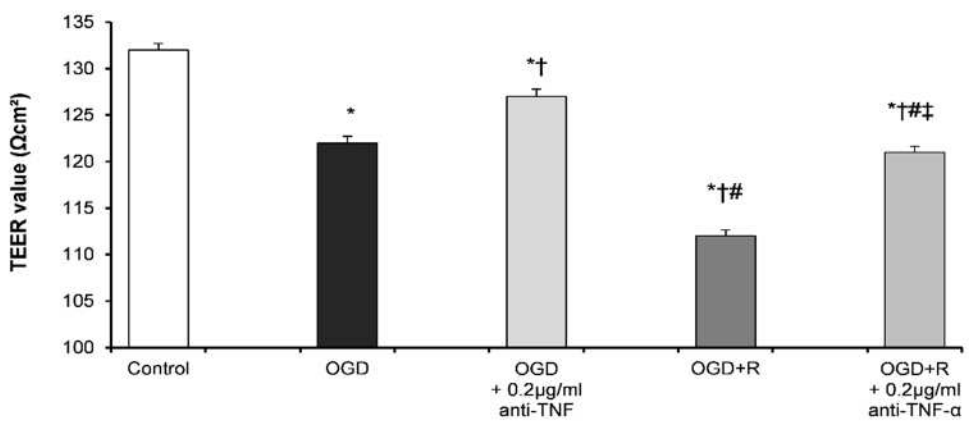

B

C

D

Figure 3

A

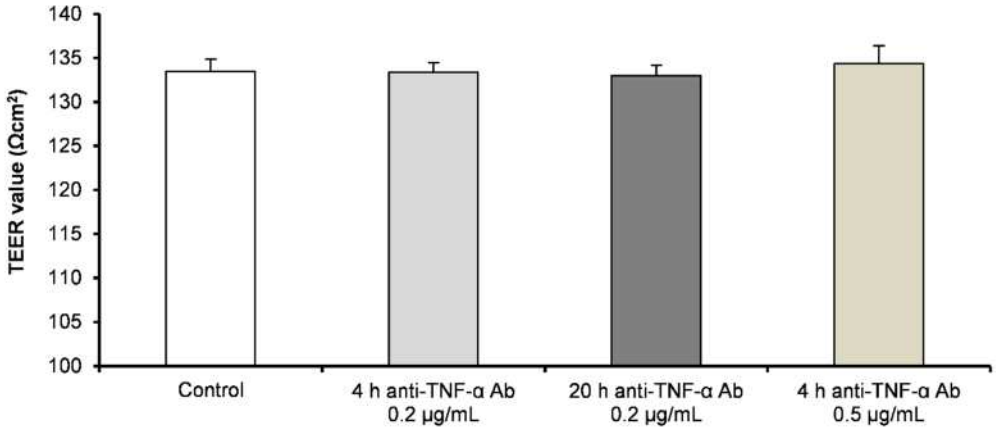

B

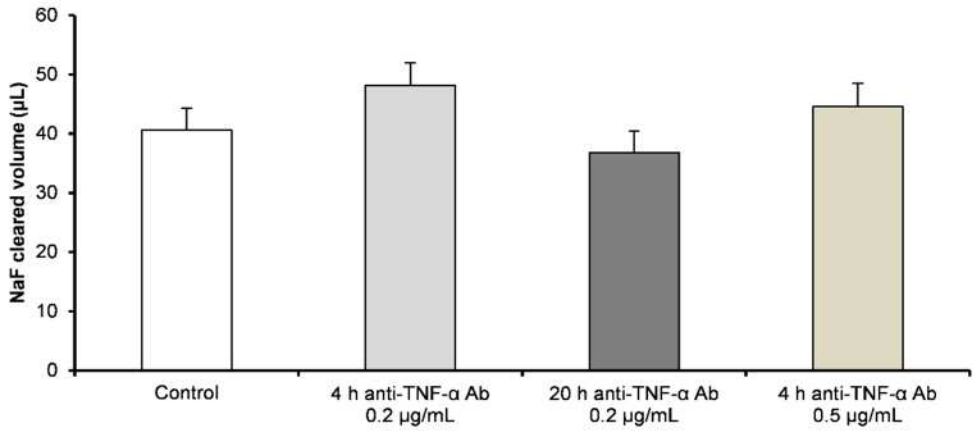
NaF cleared volume (µL)
60
50
40
30
20
10
0
Control
4 h anti-TNF-α Ab 0.2 µg/mL
20 h anti-TNF-α Ab 0.2 µg/mL
4 h anti-TNF-α Ab 0.5 µg/mL

C

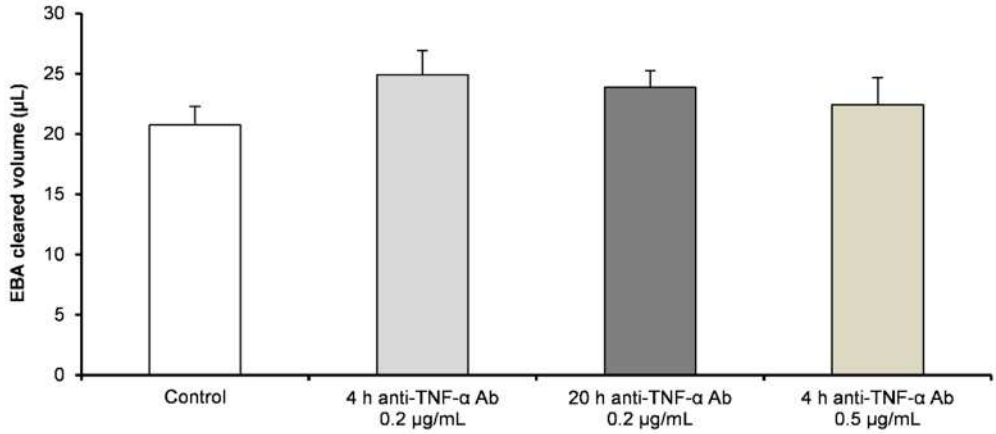
EBA cleared volume (µL)
30
25
20
15
10
5
0
Control
4 h anti-TNF-α Ab 0.2 µg/mL
20 h anti-TNF-α Ab 0.2 µg/mL
4 h anti-TNF-α Ab 0.5 µg/mL

Figure 4

A

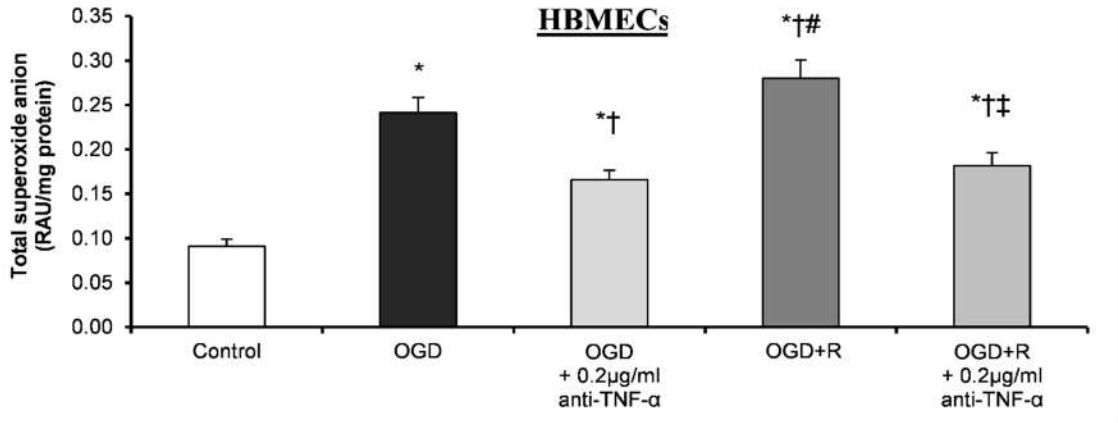
HBMECs
Total superoxide anion (RAU/mg protein)
0.35
0.30
0.25
0.20
0.15
0.10
0.05
0.00
*
*†
*†#
*†‡
Control
OGD
OGD + 0.2µg/ml anti-TNF-α
OGD+R
OGD+R + 0.2µg/ml anti-TNF-α

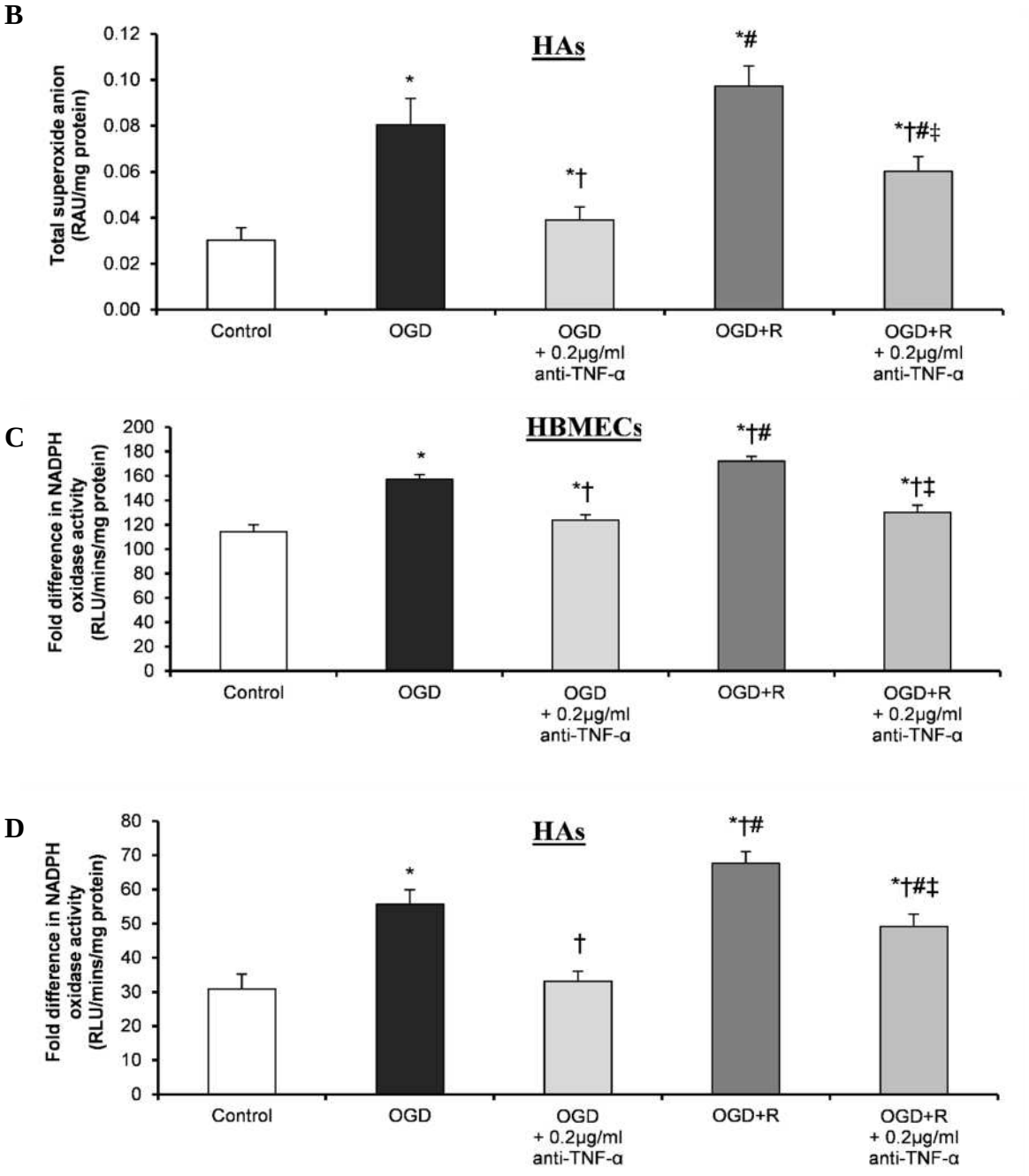
B
HAs
Total superoxide anion (RAU/mg protein)
0.12
0.10
0.08
0.06
0.04
0.02
0.00
*
*†
*#
*†#‡
Control
OGD
OGD + 0.2μg/ml anti-TNF-α
OGD+R
OGD+R + 0.2μg/ml anti-TNF-α
C
HBMECs
Fold difference in NADPH oxidase activity (RLU/mins/mg protein)
200
180
160
140
120
100
80
60
40
20
0
*
*†
*†#
*†‡
Control
OGD
OGD + 0.2μg/ml anti-TNF-α
OGD+R
OGD+R + 0.2μg/ml anti-TNF-α
D
HAs
Fold difference in NADPH oxidase activity (RLU/mins/mg protein)
80
70
60
50
40
30
20
10
0
*
†
*†#
*†#‡
Control
OGD
OGD + 0.2μg/ml anti-TNF-α
OGD+R
OGD+R + 0.2μg/ml anti-TNF-α

Figure 5

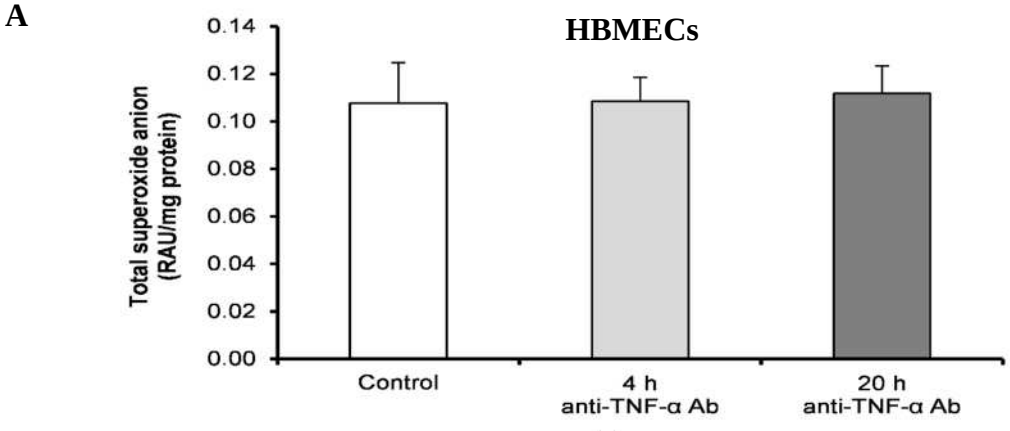
A
HBMECs
Total superoxide anion (RAU/mg protein)
0.14
0.12
0.10
0.08
0.06
0.04
0.02
0.00
Control
4 h anti-TNF-α Ab
20 h anti-TNF-α Ab

B

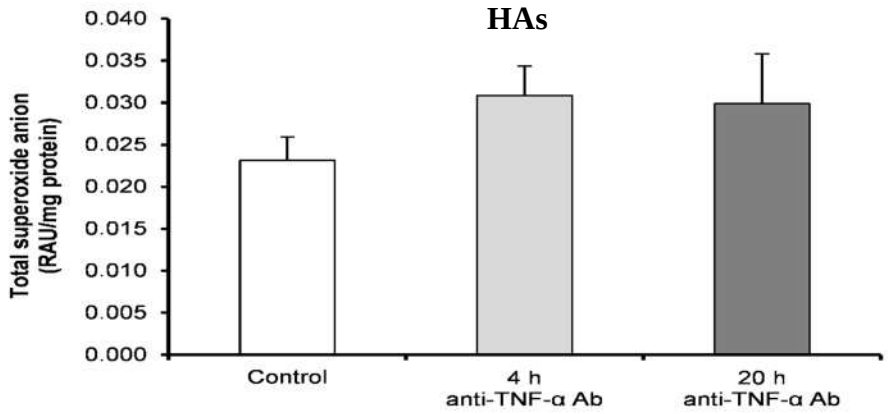

C

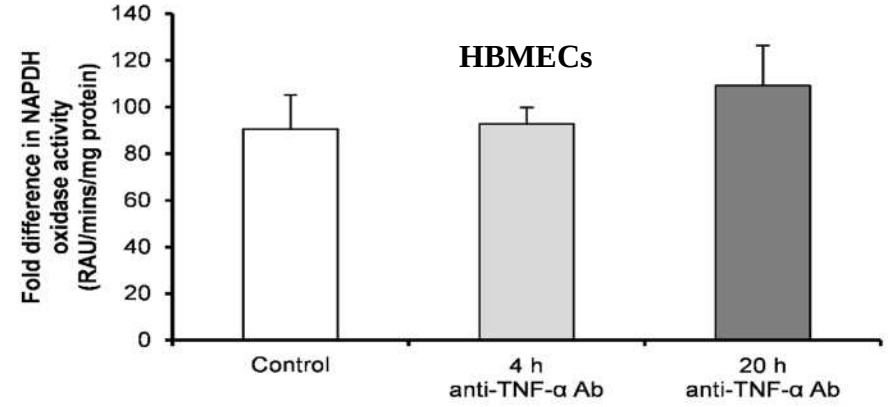

D

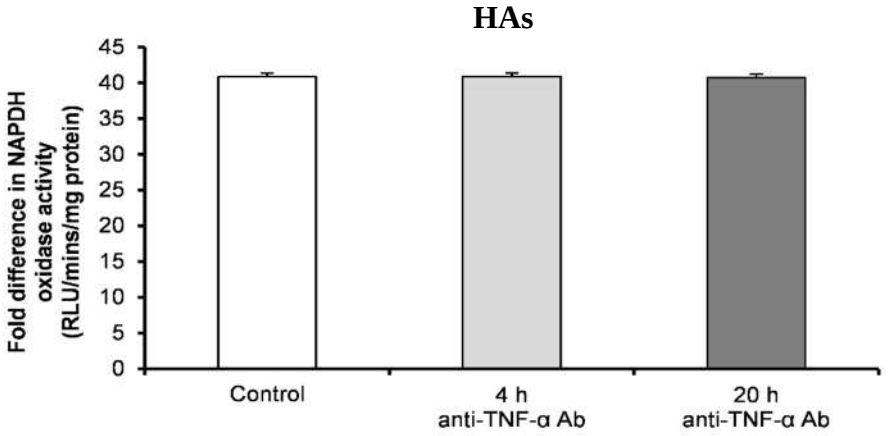

Figure 6

A **HBMECs**

Pro-MMP-2  72kDa

Pro-MMP-2  72kDa

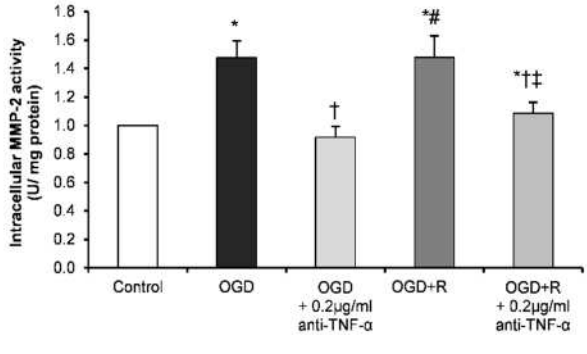

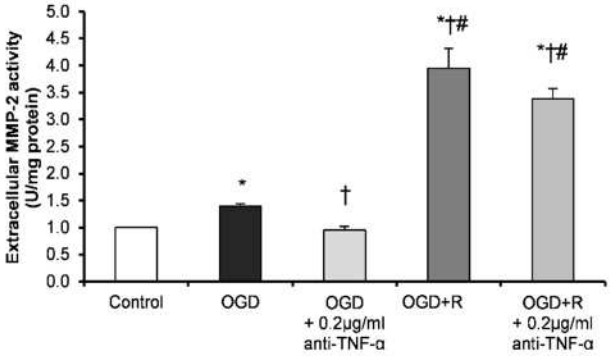

B HAs

C HBMECs

Pro-MMP-9

92kDa

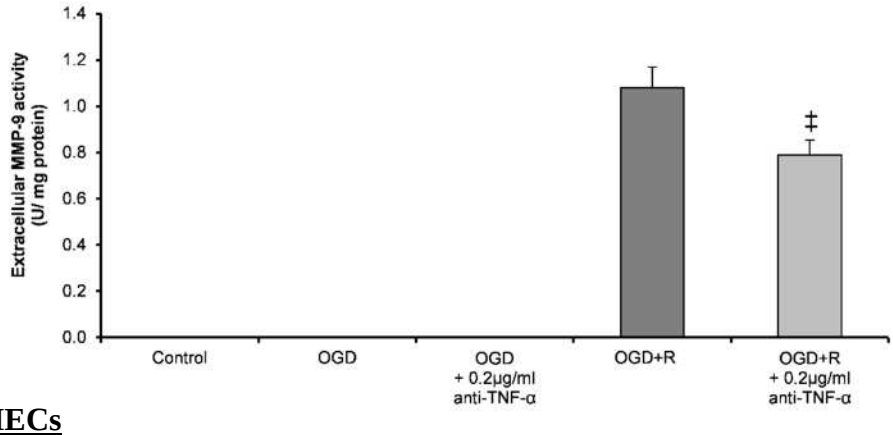

Figure 7

A HBMECs

Pro-MMP-2

72kDa

Pro-MMP-2

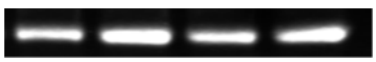

72kDa

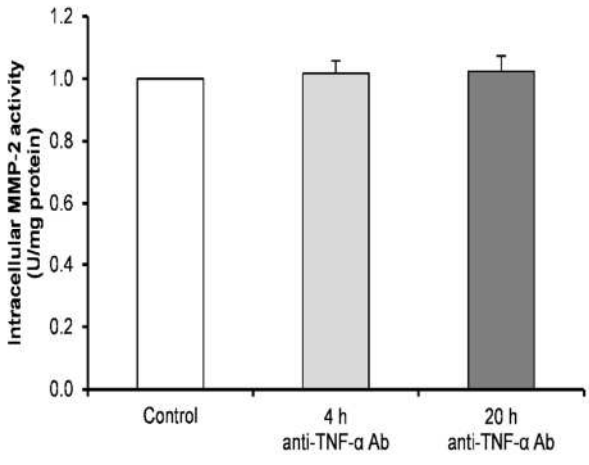

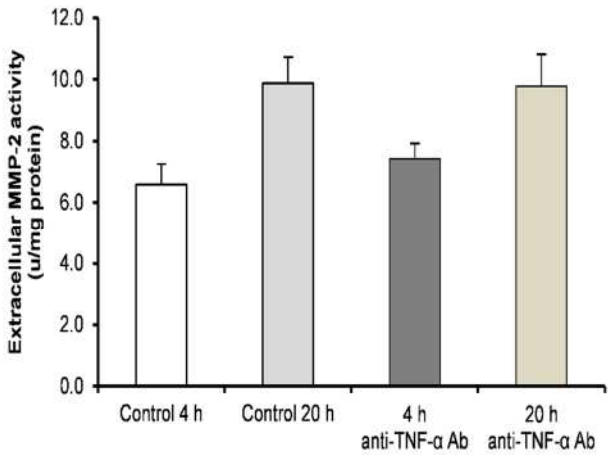

B HAs

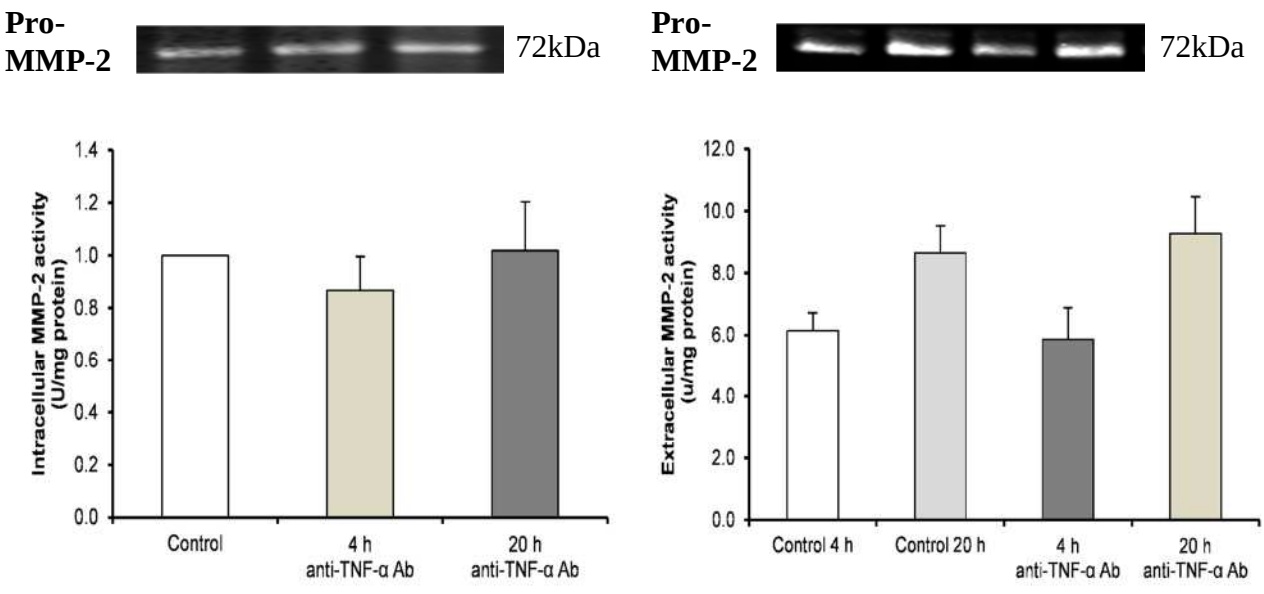

Figure 8

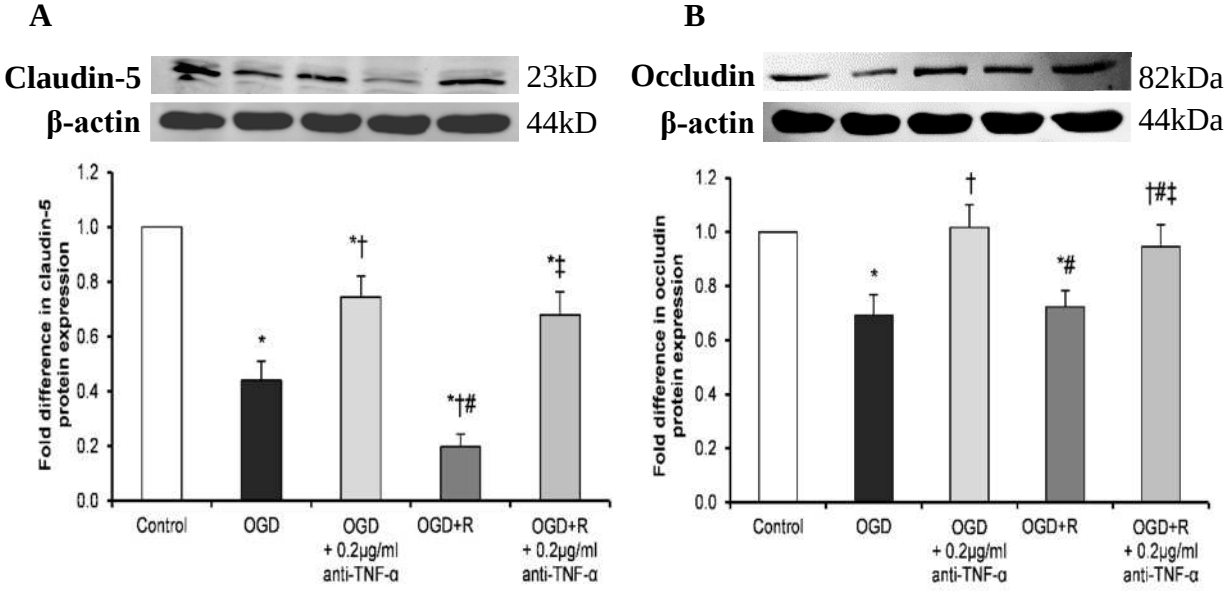

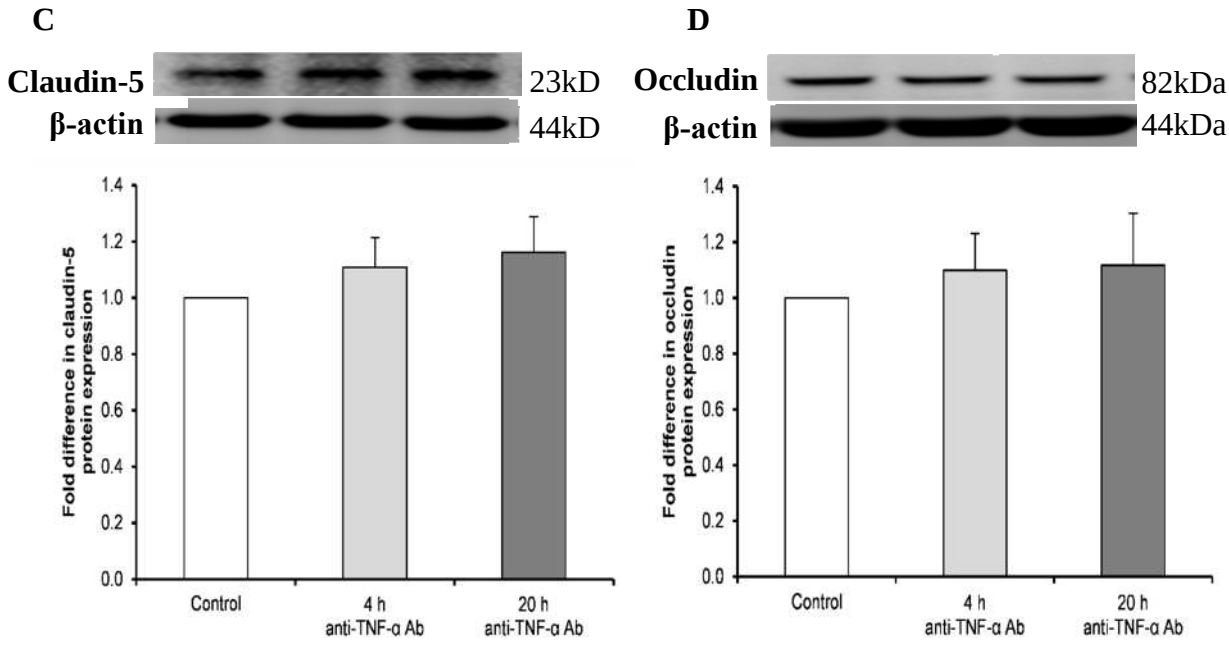

Figure 9

A **HBMECs**

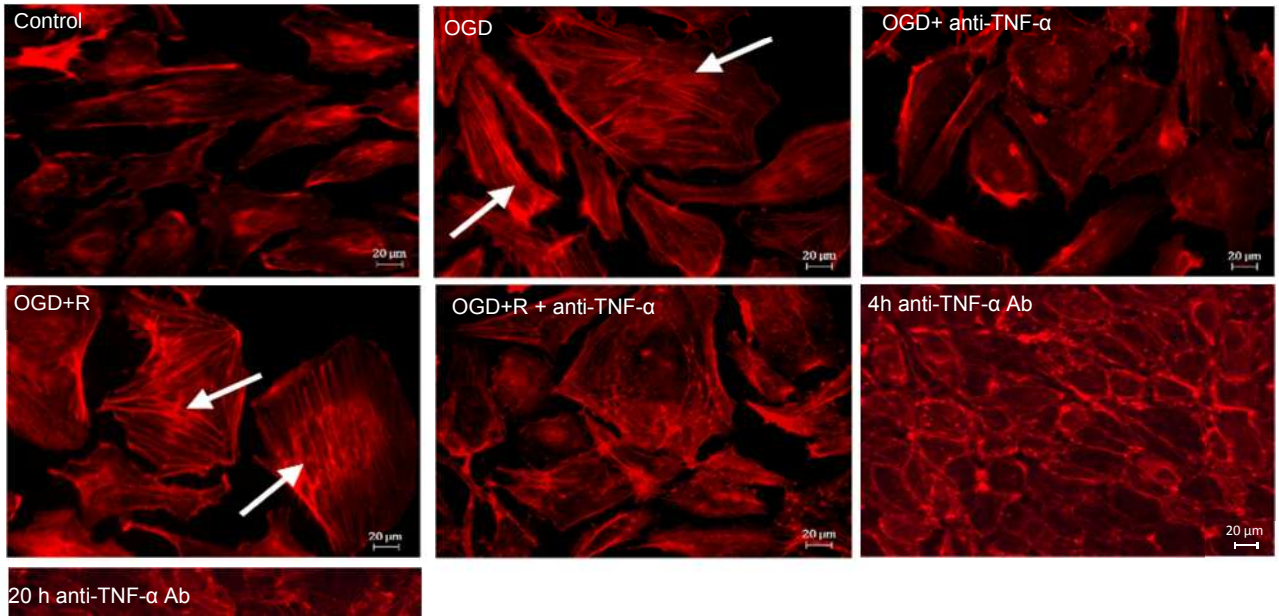

B **HAs**

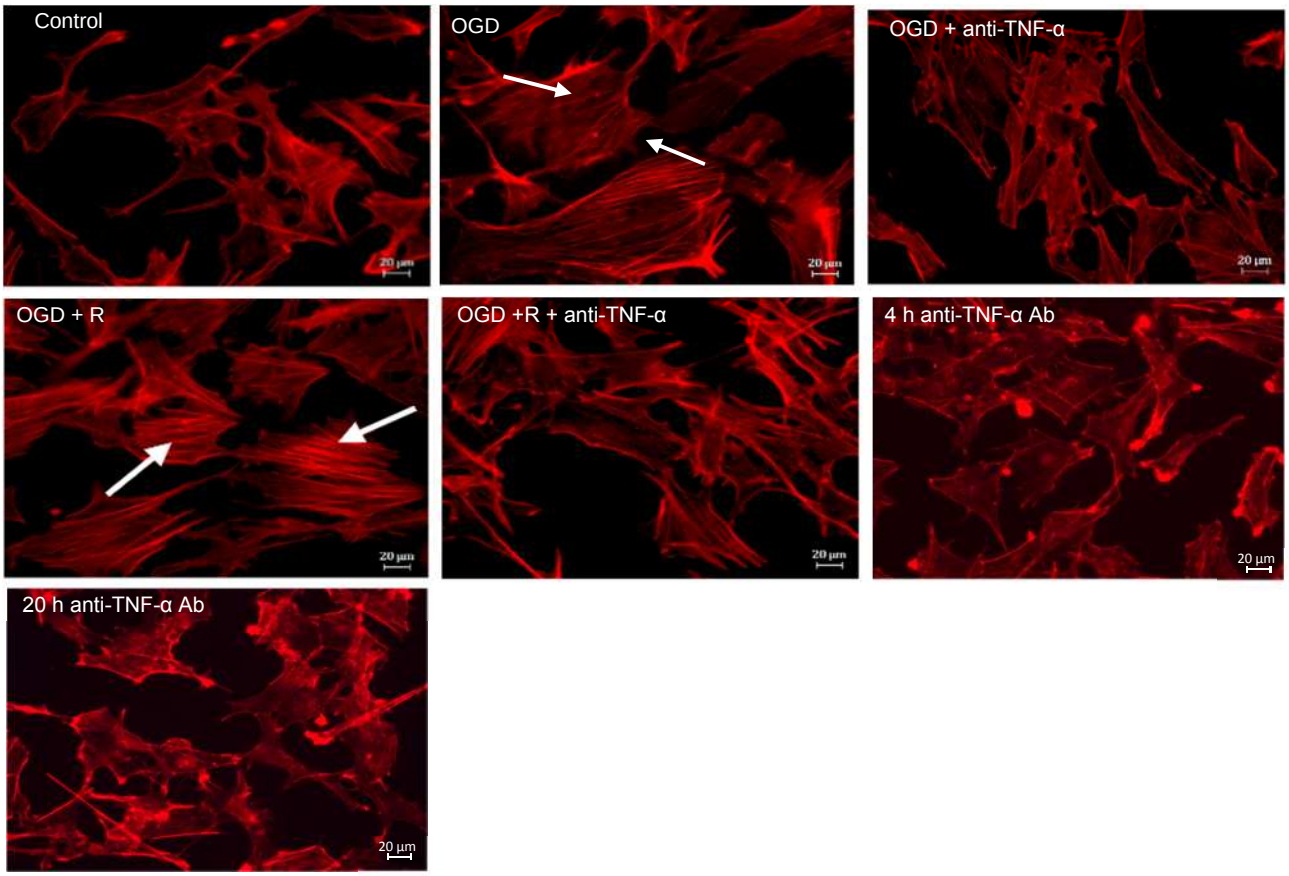

Figure 10

A **HBMECs**

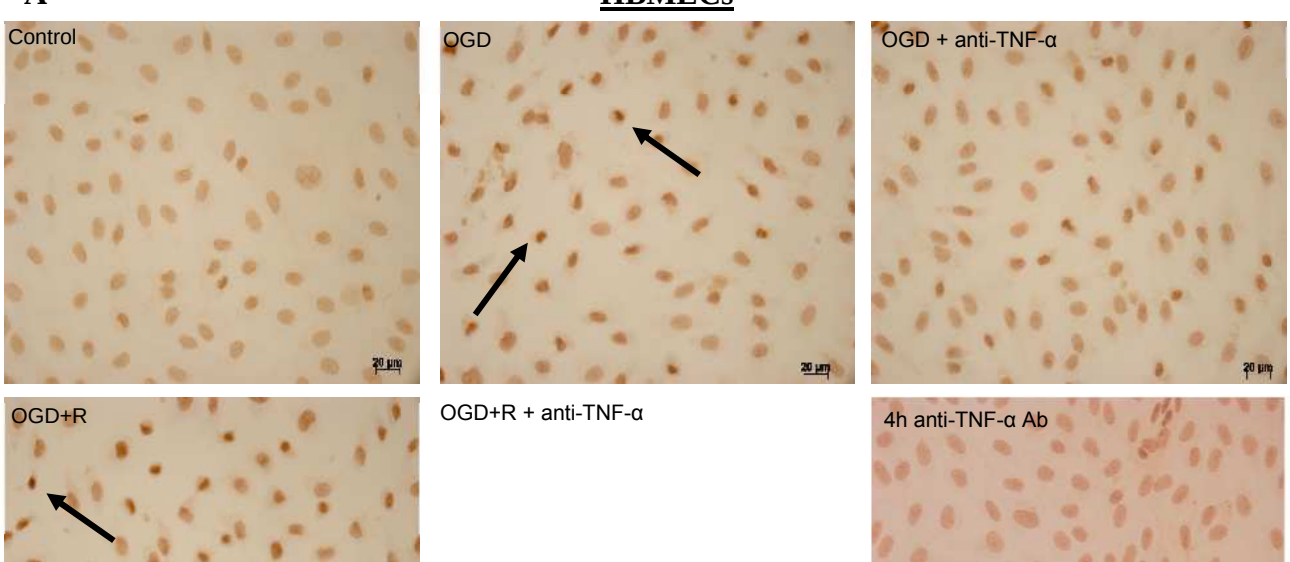

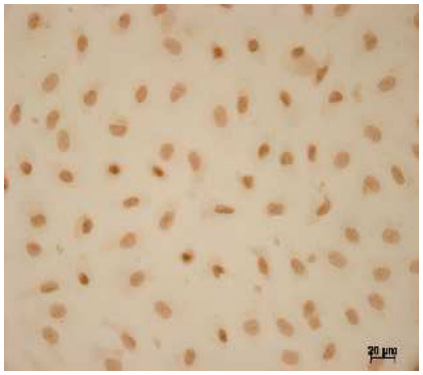

B

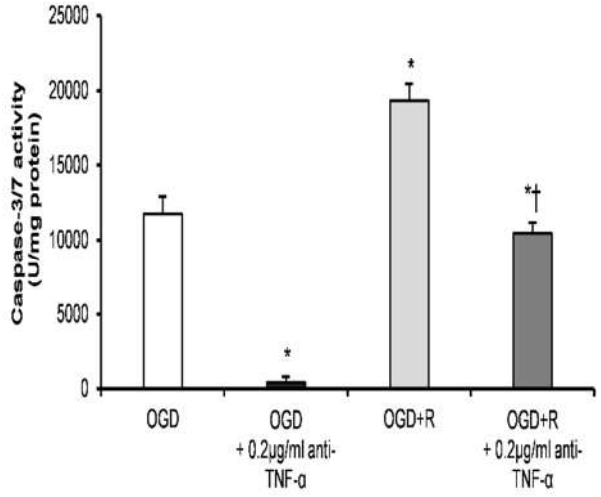

C

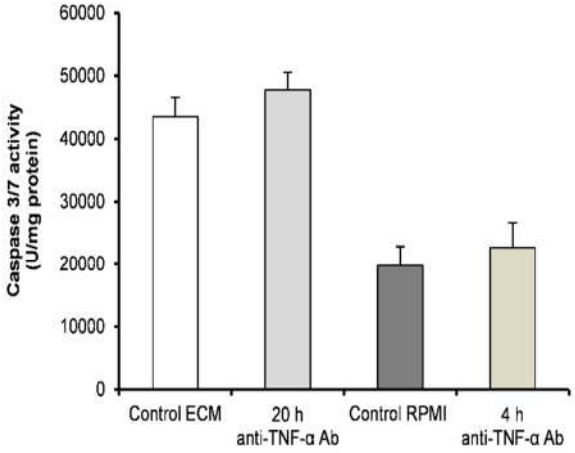

Figure 11

A

HAs

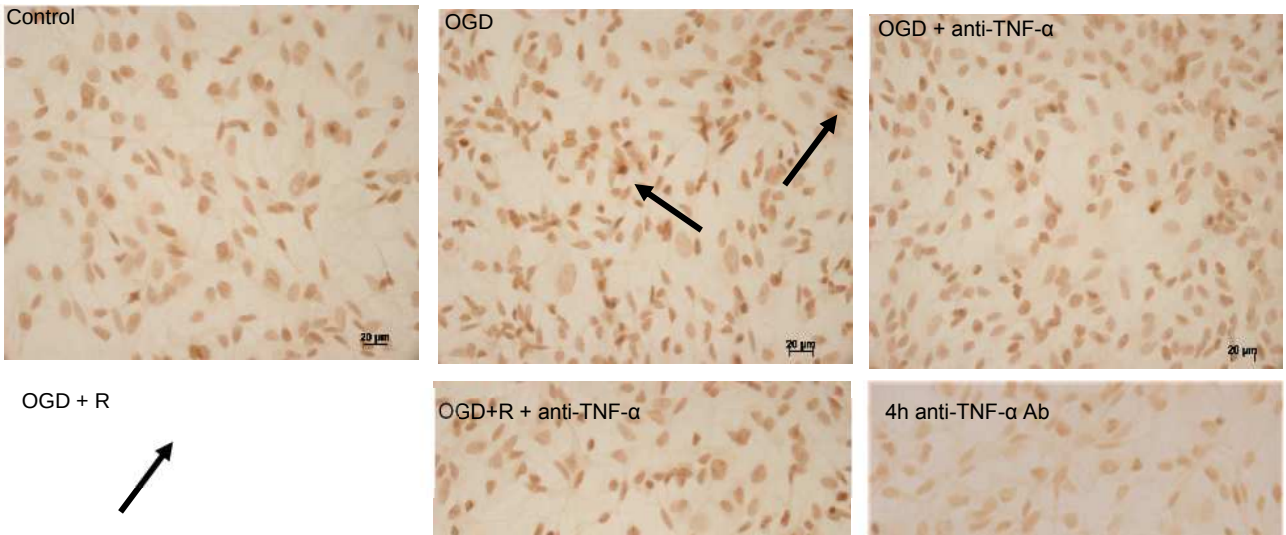

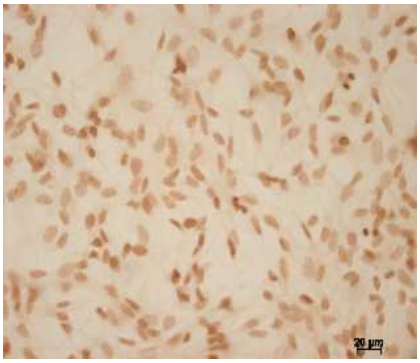

20hr anti-TNF-α Ab

B

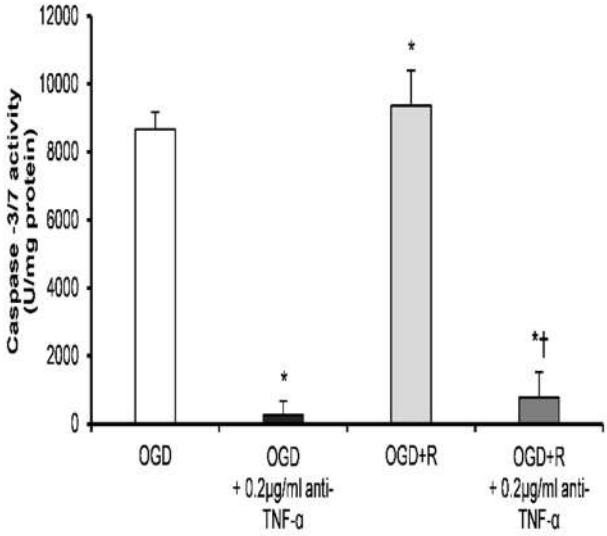

C

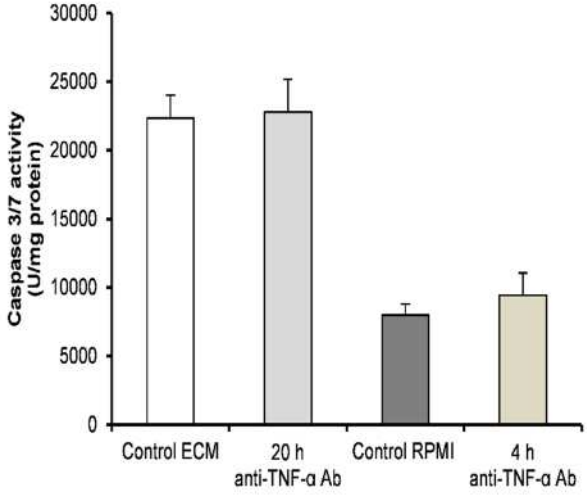

Figure 1

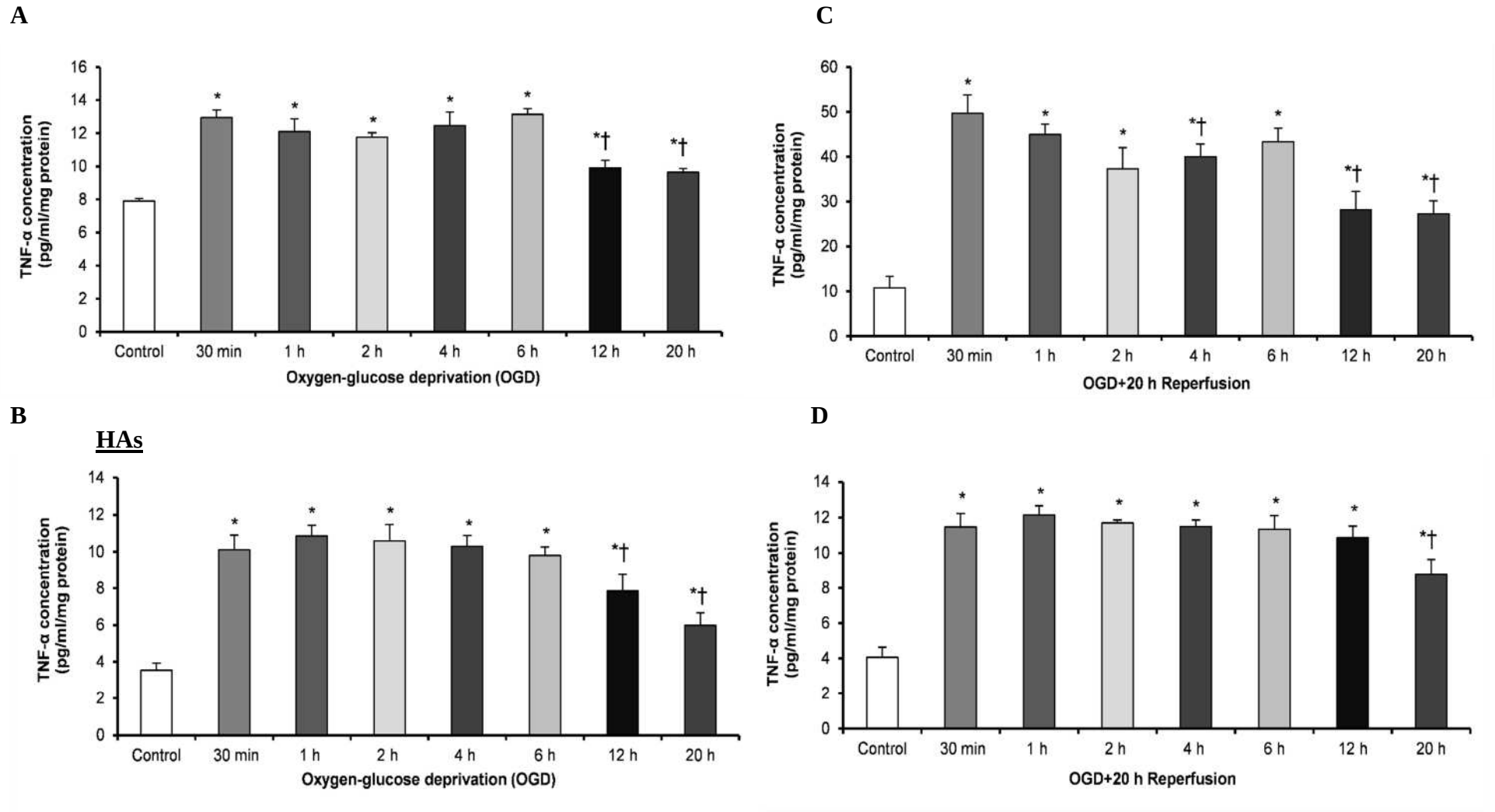
A
C
B
HAs
D
TNF-α concentration (pg/ml/mg protein)
Control
30 min
1 h
2 h
4 h
6 h
12 h
20 h
Oxygen-glucose deprivation (OGD)
OGD+20 h Reperfusion